Sediment continuity through the upland sediment cascade: geomorphic response of an upland river to an extreme flood event

Hannah M. Joyce[1]*
Richard J. Hardy[1]
Jeff Warburton[1]
Andrew R.G. Large[2]

[1]Department of Geography, Durham University, Lower Mountjoy, South Road, Durham, DH1 3LE, UK

[2]School of Geography, Politics and Sociology, Newcastle University, Newcastle Upon Tyne, NE1 7RU, UK

*corresponding author
E-mail address: hannah.joyce@durham.ac.uk (Hannah M. Joyce)

Funding: This work was supported by the Natural Environmental Research Council [grant number, NE/L002590/1]

Keywords

Sediment continuity, extreme floods, fluvial sediment budgets, upland sediment cascade, floodplain sediment storage

Highlights (3 – 5 bullets, 85 characters per bullet including spaces)

- Sediment continuity on an upland river is assessed during a 1 in 1300 year flood
- Less than 6% of sediment eroded was transported out of the valley during the event
- Sediment continuity was disrupted due to sediment storage on upland floodplains

- Channel confinement controlled the extent of flood geomorphic impacts
- Upland valley floodplains are a major coarse sediment store during extreme floods

Abstract

Hillslope erosion and accelerated lake sedimentation are often reported as the source and main stores of sediment in the upland sediment cascade during extreme flood events. While upland valley floodplain systems in the transfer zone have the potential to influence sediment continuity during extreme events, their geomorphic response is rarely quantified. This paper quantifies the sediment continuity through a regulated upland valley fluvial system (St John's Beck, Cumbria, UK) in response to the extreme Storm Desmond (4-6 December 2015) flood event. A sediment budget framework is used to quantify geomorphic response and evaluate sediment transport during the event. Field measurements show 6500 ± 710 t of sediment was eroded or scoured from the river floodplains, banks and bed during the event, with 6300 ± 570 t of sediment deposited in the channel or on the surrounding floodplains. Less than 6% of sediment eroded during the flood event was transported out of the 8 km channel. Floodplain sediment storage was seen to be restricted to areas of overbank flow where the channel was unconfined. Results indicate that, rather than upland floodplain valleys functioning as effective transfer reaches, they instead comprise significant storage zones that capture coarse flood sediments and disrupt sediment continuity downstream.

Graphical Abstract

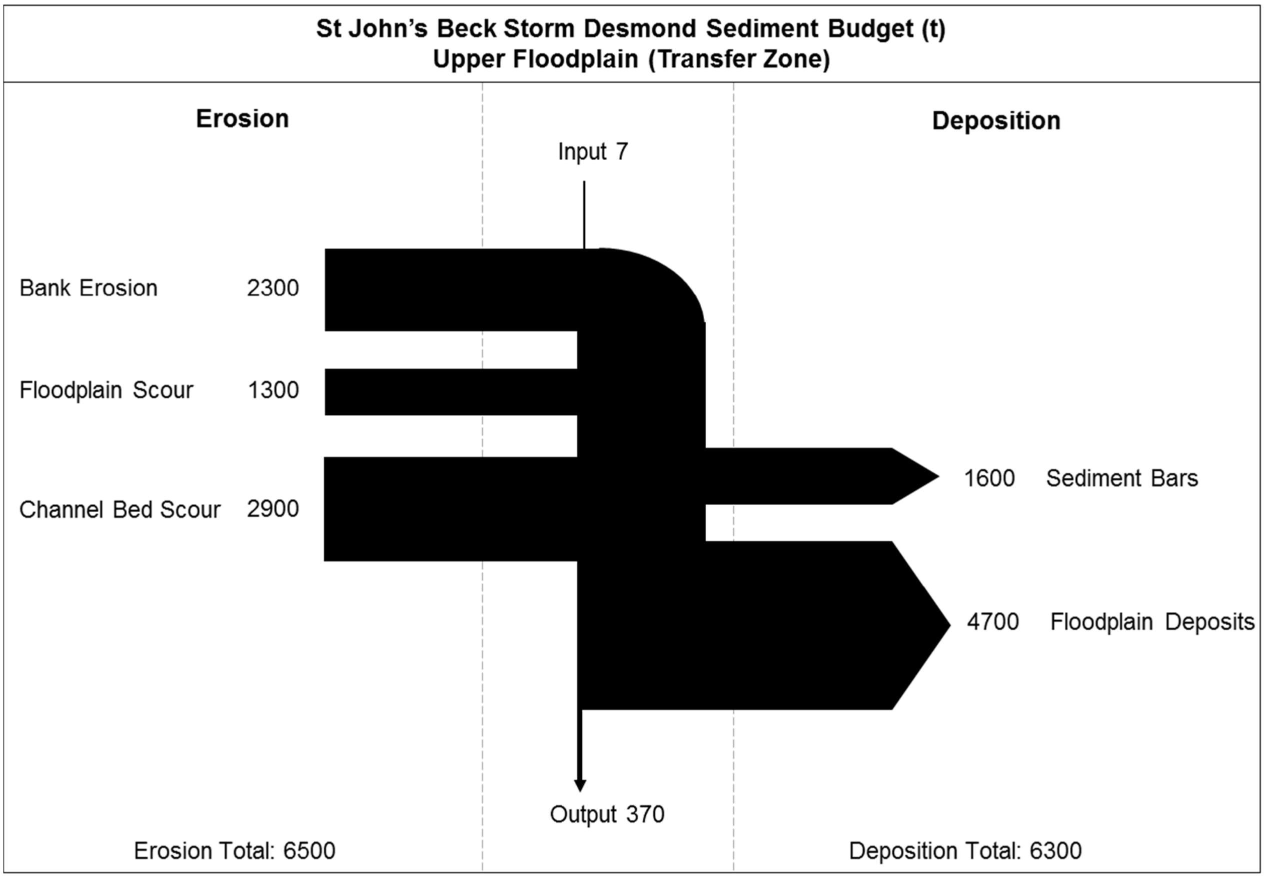

1. Introduction

Upland rivers are active geomorphic systems that generate some of the highest annual global sediment yields (Milliman and Syvitski, 1992). The steep channel gradients, high runoff and dynamic geomorphic processes result in high rates of sediment production, transfer, deposition and geomorphic change (Johnson and Warburton, 2002; Warburton, 2010). These processes are greatest during high magnitude, low frequency, extreme flood events when sediment yields can increase by orders of magnitude, even when averaged over centennial to millennial timescales (Korup, 2012; Wicherski et al., 2017). The geomorphic impacts of these extreme events such as riverbed and bank erosion (Prosser et al., 2000; Milan, 2012; Thompson and Croke, 2013), channel widening (Krapesch et al., 2011), overbank sediment deposition (Williams and Costa, 1988; Knox, 2006), floodplain scour (Magilligan, 1992) and the destruction of protection structures (Langhammer, 2010) can have significant impacts on upland river valleys and surrounding society and infrastructure (Davies and Korup, 2010). Many of these upland systems have been anthropogenically modified to minimise the geomorphic impacts of 1 in 100 yr flood events (Hey and Winterbottom, 1990; Gergel et al., 2002), but under extreme flows managed river corridors can be reactivated.

Previous research has focused on understanding the controls of such geomorphic change during extreme events to help better predict and manage the impacts. For example, studies have explored the potential for geomorphic work through magnitude-frequency relationships (Wolman and Gerson, 1978), hydraulic forces (i.e., discharge, shear stress, stream power (Magilligan, 1992; Thompson and Croke, 2013)), catchment characteristics such as valley confinement (Righini et al., 2017), the role of engineered structures (Langhammer, 2010) and anthropogenic modifications (Lewin, 2013). However, only a few studies (Trimble, 2010; Warburton, 2010; Warburton et al., 2016) have investigated the geomorphic impacts of extreme events in terms of sediment continuity of the upland catchment sediment cascade (USC). Here, sediment continuity is defined as the physical transfer or exchange of sediment from one part of the fluvial system to another, and represents the conservation of mass between sediment inputs, stores and outputs. Sediment continuity is therefore distinct from the concept of sediment connectivity (Hooke, 2003; Bracken et al., 2015) as it describes the pathways for sediment transfer by quantifying the physical movement and storage of sediment mass.

The USC describes the supply, transfer and storage of catchment sediment from source to sink (Chorley and Kennedy, 1971; Slaymaker, 1991; Burt and Allison, 2010). Figure 1 provides a framework for the USC displaying the main sediment stores that are often characterised in upland sediment budget studies (Reid and Dunne, 1996; Fuller et al., 2002; Brewer and Passmore, 2002). The USC is adapted from Schumm's (1977) simple sediment cascade (SSC) model that divides the fluvial system into the production zone, transfer zone and deposition zone. In many upland regions however, the SSC is modified due to the presence of water bodies such as lakes, reservoirs or impoundments, which restrict sediment continuity between zones (Foster, 2010). Many of these water bodies (>40%) are the product of previous glacial activity that has scoured over-deepened basins (Herdendorf, 1982; Foster, 2010; McDougall and Evans, 2015). These basins occur both towards headwaters, between catchment production and transfer zones, as well as in lowland reaches where they form major long term depositional sites (Petts, 1979; Williams and Wolman, 1984; Kondolf, 1997). The movement of coarse sediment in and between the zones of the USC has been compared to a 'jerky conveyor belt' (Ferguson, 1981; Newson, 1997) where sediment is transferred and stored over a range of temporal scales. Sediment stores can fuel or buffer sediment transport rates and therefore influence sediment continuity and potential geomorphic change downstream; this is particularly relevant during less frequent higher magnitude events where sources and stores of sediment can rapidly change over a short period of time (Davies and Korup, 2010; Fryirs, 2013).

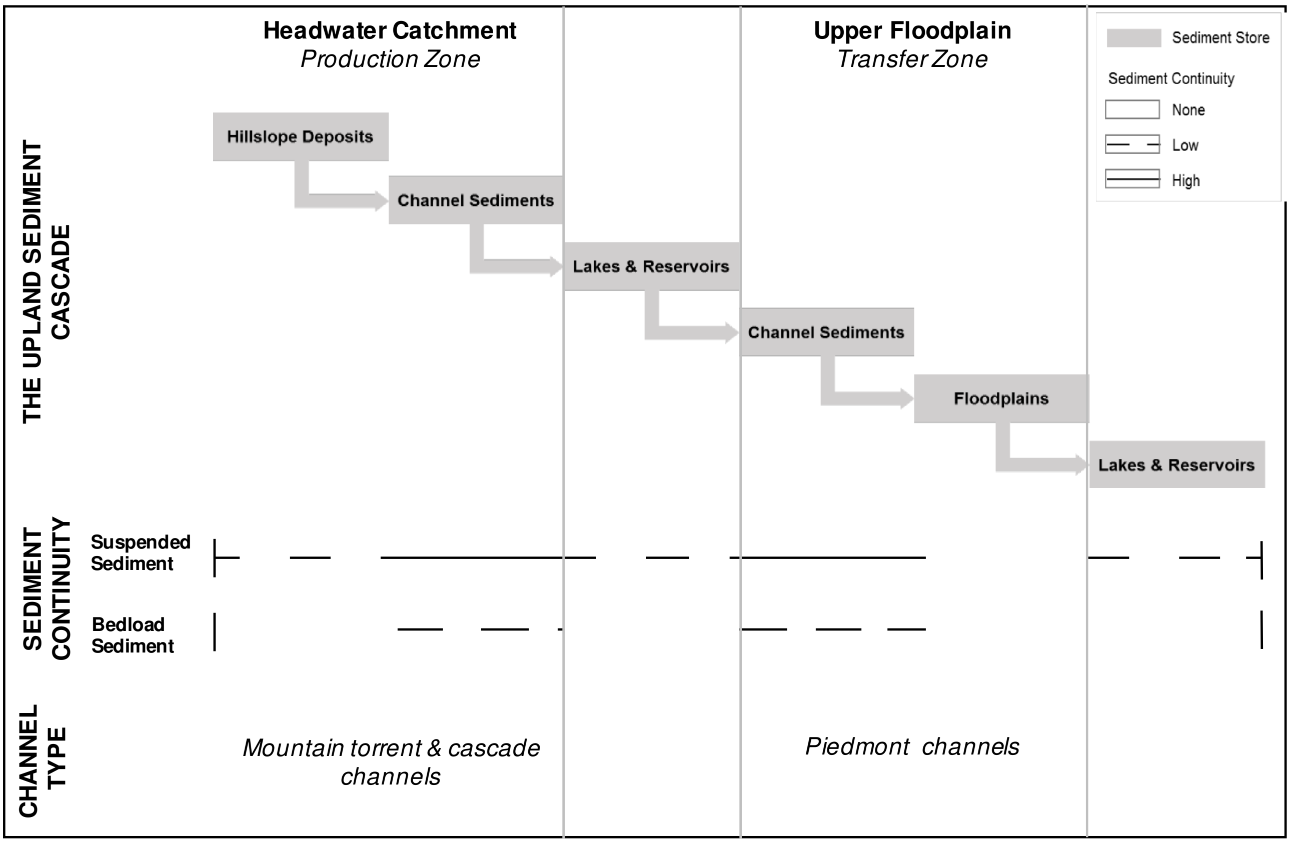

Fig. 1. The upland sediment cascade (USC) framework displaying sediment stores and the relative sediment continuity through each store during non-flood conditions. The USC framework is modified from Schumm's (1977) Simple Sediment Cascade model.

The USC production zone is characterised by mountain torrent and cascade channels that have steep channel slopes (>0.03-0.30) and surrounding hillslopes (>0.15-0.7) (Montgomery and Buffington, 1993). Here, channels are confined by the local valley topography and have no intervening floodplain; hillslopes are strongly (>80%) coupled to the channel (Lewin, 1981; Montgomery and Buffington, 1993; Harvey, 2001; Korup, 2005; Crozier, 2010). Sediment flux in this zone is dominated by suspended sediment, but during flood events bedload and coarse sediment stored on hillslopes can be mobilised, thus contributing to the total sediment load (Ashbridge, 1995). Hillslope erosion processes (mass wasting or water-driven) are the principal sources of sediment, which is deposited either on the hillslopes or in the channel (Montgomery and Buffington, 1993; Fuller et al., 2016). Previous studies have explored sediment dynamics in the USC production zone including: (i) hillslope-channel coupling relationships (Harvey, 2001, 2007; Johnson et al., 2008; Smith and Dragovich, 2008; Caine and Swanson, 2013), (ii) variability in sediment supply, transfer and deposition (Johnson and Warburton, 2006), (iii) response of these systems to extreme flood events (Johnson and Warburton, 2002) and (iv) the relative contribution of sediment sources to the channel through sediment budgeting approaches (Warburton, 2010).

In contrast, in the transfer zone (Fig. 1), sediment sources and deposits differ from those of the production zone as the channel (or piedmont channel) gradient decreases (slopes of <0.001-0.03), floodplain width increases, and the channel becomes unconfined allowing greater channel-floodplain interaction (Lewin, 1981; Church, 2002). Hillslope erosion processes are disconnected from the active channel by floodplains and therefore do not contribute directly to channel sedimentation (Lewin, 1981; Church, 2002). Instead, sediment in this zone is sourced from tributary inputs and reworked from channel bed and bank deposits. Suspended sediment dominates the low to medium flow sediment fluxes, with bedload sediment stored in the channel only mobilised at 50-60% of bankfull flow (Carling, 1988; Knighton, 1998; Fuller et al., 2002). Only during overbank flow is the largest bedload sediment entrained in quantity in this zone (Carling, 1988). Sediment continuity in the transfer zone is heavily influenced by anthropogenic modifications to the system (Fryirs et al., 2007; Lewin, 2013). The presence of upstream reservoirs or impoundments disrupt coarse sediment supply from headwaters, and influence the potential for sediment transport downstream through flow regulation (Petts and Thoms, 1986; Kondolf, 1997). Many of these systems have become 'genetically modified' over time (Lewin, 2013) with channels artificially confined by flood protection structures to safeguard adjacent land, reducing channel-floodplain interactions. Consequently, sediment continuity and potential for sediment storage on the floodplains during extreme flood events is heavily modified by anthropogenic activity (Wohl, 2015).

Previous research has discussed the impacts of lakes, dams and impoundments on downstream sediment transport in the USC transfer zone (Gurnell, 1983; Kondolf, 1997; Petts and Gurnell, 2005). More recently, Sear et al. (2017) modelled the response to the 2009 and 2015 Cumbria floods on the Lower River Derwent, downstream of Bassenthwaite Lake, showing how the modified confined channel reverted to a course dictated by the wider valley morphology. However, the continuity of sediment transfer through intervening modified valley systems has only rarely been directly surveyed or evaluated in detail after extreme flood events (i.e., Johnson and Warburton 2002; Warburton, 2010) and few studies have looked at how these systems recover following these extremes (Milan, 2012).

Understanding sediment continuity during extreme events in upland valley systems will become increasingly important for hazard management given projected increases in winter precipitation from predicted climate change (Raven et al., 2010; van Oldenborgh et al., 2015). However, extreme flood events are difficult to predict (Lisenby et al., 2018) and there are few direct measurements from these events. Consequently, their impacts have to be inferred from historical information and estimates of the quantity of sediment stored and transported are generally poorly constrained.

This paper quantifies the geomorphic response of an upland river valley system (transfer zone) to Storm Desmond, an extreme flood event that hit Cumbria, Northwest UK in December 2015. Specifically we (i) quantify the geomorphic impacts of the extreme event on the upper floodplain valley system of the USC; (ii) estimate bedload sediment transport rates during the flood; (iii) evaluate system recovery one year after the flood event and (iv) place findings within the wider context of sediment continuity through the USC. This study is the first to quantify the role of the floodplain zone in the USC in response to an extreme event and thus will enable better understanding of sediment continuity in upland regions.

2. Study site

This study focused on St John's Beck, an 8 km channelised, regulated gravel bed river downstream of Thirlmere Reservoir, Central Lake District, UK (OS National Grid Reference (NGR): NY 318 203, catchment area including Thirlmere Reservoir is 53.4 km^2, effective catchment area is 12 km^2) (Fig. 2a). St John's Beck is a tributary to the River Greta that flows through the town of Keswick before discharging into Bassenthwaite Lake (area = 5.1 km^2). St John's Beck ranges in altitude from 178 m OD at the Thirlmere Reservoir outlet to 130 m OD where it joins the River Greta (Fig. 2a). St John's Beck lies in the upper floodplain transfer zone of the USC (Fig. 2b). The channel has a Strahler (1952) stream order of 3, mean channel slope of 0.005 and mean channel width of 12 m. St John's Beck lies in a glaciated valley (Vale of St John's) that is underlain by Ordovician Borrowdale Volcanic rocks in the north of the catchment and the Skiddaw group in the south. The land surrounding the channel is predominantly mixed woodland and pasture used for livestock grazing. St John's Beck is a Site of Special Scientific Interest and lies in the Derwent and Bassenthwaite Lake Special Area of Conservation. The river is protected to support salmon, lamprey species, otters and floating water plantain (Wallace and Atkins, 1997; Reid, 2014).

St John's Beck has a wandering planform which has been restricted laterally due to channelisation in the late nineteenth century following the impoundment of Thirlmere Reservoir (area = 3.3 km^2). The channel is confined by the natural valley topography in the upstream reaches. Floodplain valley width increases 1.8 km downstream from Thirlmere Reservoir (Fig. 2a), however the river channel has been modified and restricted from movement here (1.8-5 km downstream) through bank reinforcement and flood protection levees. Flood protection levees were built to protect farmland and a major link road from flooding. Long term flow regulation has influenced sediment transport rates in St John's Beck and as a result the system displays clear zones of aggradation. There are four first order tributaries that flow into St John's Beck. Flow and sediment are intercepted from two of these tributaries, which drain the Helvellyn mountain range and are directed to Thirlmere Reservoir (Reid, 2014; Bromley, 2015). The third and fourth first order tributaries are constrained by the presence of a road and a sediment trap and therefore are not a major source of sediment to St John's Beck.

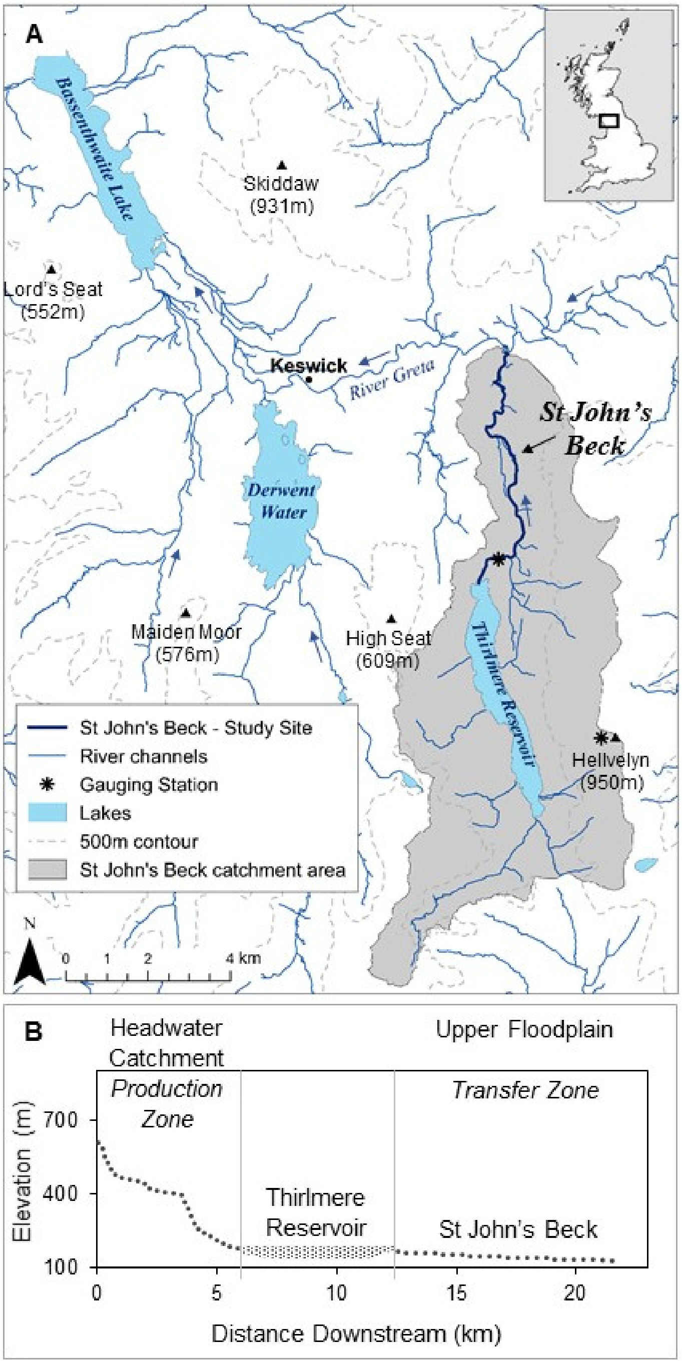

Fig. 2. (A) Location and catchment area of St John's Beck, Cumbria, UK, identifying the study reach and catchment discharge and rainfall gauging stations. Arrows indicate flow direction. (B) Long profile through the St John's Beck catchment showing the interruption of Thirlmere Reservoir on the USC.

3. The Storm Desmond flood event

Extreme flood events in the Lake District have been documented from 1690 to the present (Watkins and Whyte, 2008) (recent floods summarised in Table 1). This study describes the geomorphological impacts of the Storm Desmond (4-6 December 2015) flood event. Storm Desmond, a North Atlantic storm, was associated with a mild and moist slow moving low pressure system located northwest of the UK that brought severe gales and exceptionally persistent heavy rainfall over northern UK (Met Office, 2016). Northern England experienced the wettest December on record (in a series from

1910), following the second wettest November, after 2009 (McCarthy et al., 2016). The average December rainfall doubled in northern England, with the Lake District receiving three times its average monthly rainfall (McCarthy et al., 2016). Storm Desmond produced record-breaking rainfall maximums in the UK: 341.4 mm rainfall was recorded in a 24 h period at Honister Pass (NGR NY 225134), Western Lake District, and 405 mm of rainfall was recorded in a 38 h period at Thirlmere (study catchment), central Lake District (NGR NY 313 194). The storm was the largest in the 150 yr local Cumbrian rainfall series (1867 – 2017), and exceeded previous records set in the 2005 and 2009 Cumbrian floods. The estimated return period for the rainfall event was 1 in 1300 years (CEH, 2015) based on the FEH13 rainfall frequency model (Stewart et al., 2014). The UK climate projection change scenarios for northwest England predict winter flood events like this will occur more often in the future because of increases in rainfall intensity due to climate change (Watts et al., 2015).

3.1. Storm Desmond impacts

Storm Desmond caused widespread disruption across northern England, and in particular in upland areas in the Lake District region. The event captured national attention when extreme weather conditions prompted a full scale emergency response to extreme flooding, erosion and sediment movement by upland rivers. Over 5000 homes were flooded, access routes were destroyed (257 bridges destroyed) and key infrastructure was affected, including the erosion of the main A591 trunk road through the central Lake District. The latter was estimated to cost the local economy £1 million per day (BBC, 2016). In the production zone of the USC, saturated hillslopes and high porewater pressures triggered landslides in a number of valleys, with sediment eroded and transported through mountain torrents (Warburton et al., 2016). Geomorphic impacts in the upper floodplain system of the USC included the erosion of riverbed and banks, floodplain scour, scour around man-made structures (bridges, levees) and extensive deposition of coarse sediment across floodplains. Storm Desmond caused severe flooding and substantial geomorphic change along St John's Beck (Fig. 3).

Date of Event	Rainfall (mm) in 24-h period	Estimated 24-h Rainfall Return Period (yr)	Reference
31 January 1995	163.5	80	Johnson and Warburton (2002)
7-8 January 2005	173	100	Roberts et al. (2009); Environment Agency, (2006)
18-20 November 2009	316.4	480	Sibley (2010); Stewart et al. (2010); CEH (2015)
Storm Desmond, 4–6 December 2015	341.4	1300	CEH (2015)

Table 1 Recent flood events in Cumbria, UK, including the 24-h rainfall total and 24-h rainfall return period.

Fig. 3. Photographs of the impacts of Storm Desmond along St John's Beck and the surrounding floodplains. (A–B) Flood sediments and debris (tree trunks) transported and deposited on floodplains and in the channel. (C–D) Floodplain scour. (E) Riverbank erosion. (F) Destruction of the access bridge over St John's Beck to Low Bridge End Farm (bridge approximately 3.5 m high for scale).

3.2. Hydrological regime in St John's Beck

Flooding is not unusual in St John's Beck, historic accounts describe a "most dreadful storm… with such a torrent of rain, [which] changed the face of the country and did incredible damage in [St John's in the Vale]" in 1750, (Smith, 1754). This historical event has characteristics similar to that of Storm Desmond, with large boulders of sediment being transported and deposited on floodplains along the transfer zone. Long term rainfall records available for the St John's Beck Catchment (Fig. 4a, Helvellyn Birkside gauging station NGR NY 338 133, ~6.3 km south of St John's Beck; Fig. 1) show Storm Desmond contributes to the greatest monthly rainfall event (1361 mm rainfall in December 2015) being five times higher than the mean December rainfall total in the 150 yr time series. The rain gauge on St John's Beck (NGR NY 313 195; Fig. 1) shows the rain that fell during December 2015 fell on previously saturated ground, following a total of 559 mm in November 2015 (Fig. 4b). These antecedent conditions comprise the second wettest November recorded at this site after the 2009 floods (Met Office, 2016). Daily rainfall totals (Fig. 4c) show the event peaked on 5 December 2015, where over a 15 min peak period, an estimated 6.8 mm of rain was recorded. Discharge records for St John's Beck (Fig. 5a) similarly show Storm Desmond was the largest magnitude event in the 82 yr flow record with an estimated peak discharge recorded during the event of 75.4 $m^3 s^{-1}$ (Fig. 5b). Mean discharge for St John's Beck during the 82 yr record period is 0.85 $m^3 s^{-1}$; in 2015 mean discharge was 2 $m^3 s^{-1}$.

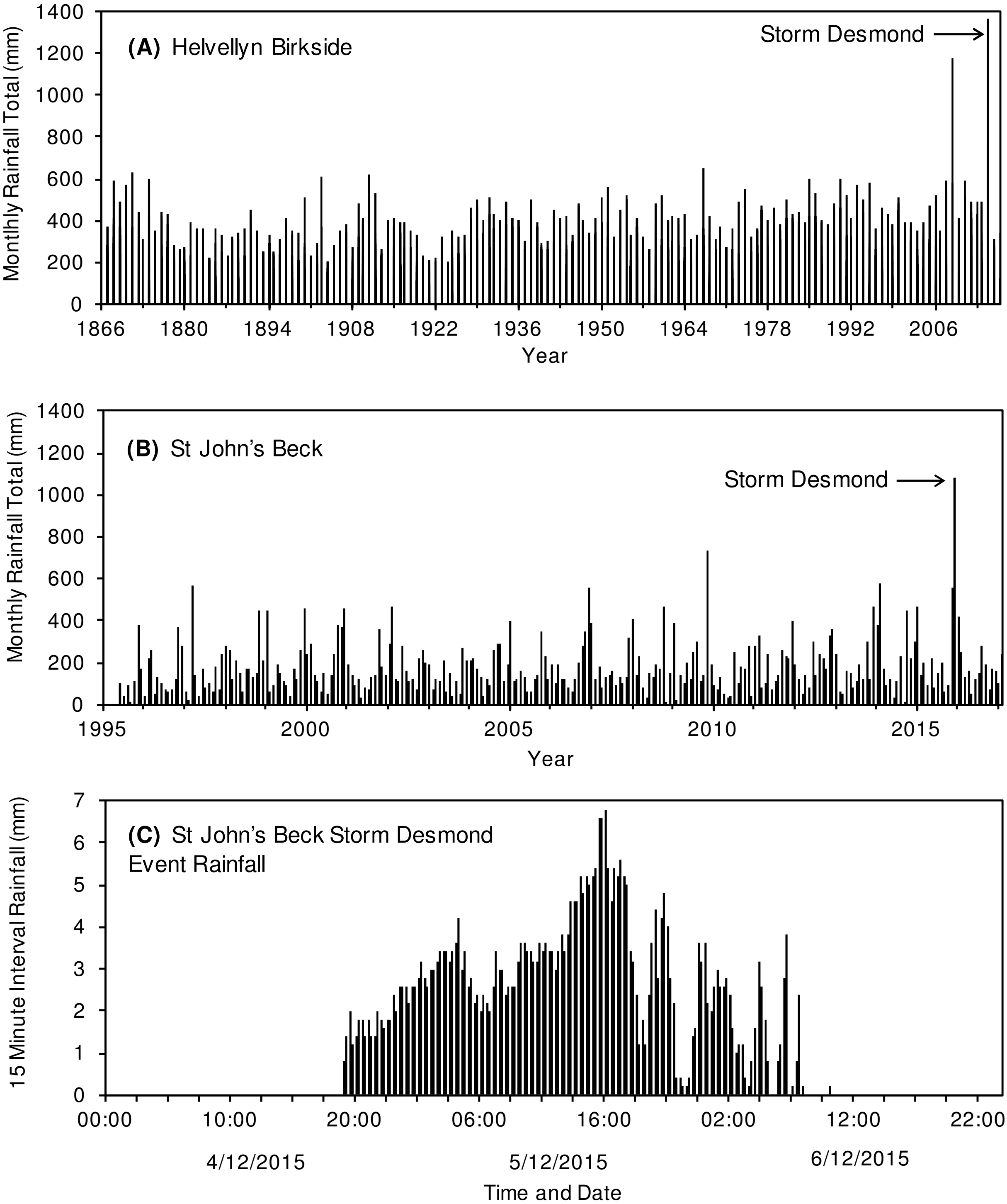

Fig. 4. Rainfall records in the St John's Beck catchment. (A) Long term (1860 – 2017) monthly rainfall variability in the St John's Beck catchment from the Helvellyn Birkside rain gauge (NGR NY 338 133). (B) Monthly rainfall totals from the St John's Beck Environment Agency (EA) tipping bucket rain gauge (TBG) from 1995-2017. (C) 15 min interval rainfall record from St John's Beck EA TBG (NGR NY313 195) during the Storm Desmond flood event.

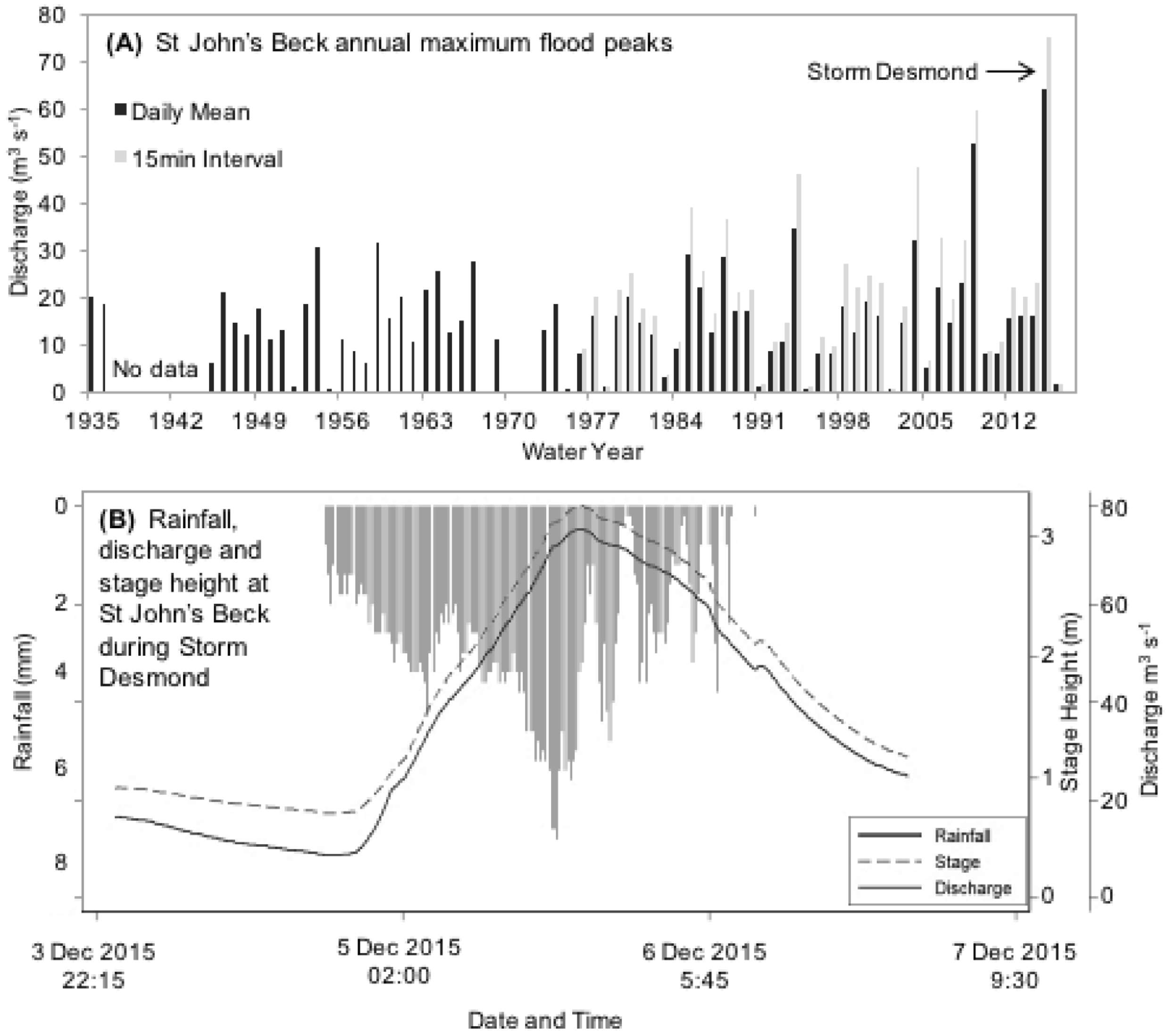

Fig. 5. Discharge records for St John's Beck gauging station. (A) Annual maximum flood peaks for St John's Beck gauging station 1935-2016 using daily mean and 15 min interval recorded flow data. (B) Estimated discharge, stage height and total rainfall during Storm Desmond.

4. Methods

This study analyses geomorphic data collected during two field campaigns at St John's Beck. The first survey was completed after the Storm Desmond flood (April-May 2016) to capture the geomorphic impacts of this event before clean-up operations and reworking of flood sediments occurred. The second survey was conducted in June 2017 to assess short-term system recovery following the flood. All field data were digitised and analysed in a GIS in British National Grid coordinates. A 5 m resolution digital elevation model (DEM) (Edina Digimap, 2016), pre-flood aerial imagery, 2009-2011, (from Bluesky International Limited, resolution 0.25 m) and post-flood event, May 2016, (from the Environment Agency, resolution 0.2 m) were used for validating field measurements and to assess valley topographic and local controls of the geomorphic impacts observed.

4.1. Geomorphic analysis

4.1.1. Channel geometry and bed material

A Leica Geosystems Real Time Kinetic differential GPS (RTK dGPS) 1200, was used to survey channel cross section geometry, floodplain geometry and thalweg long profile during the 2016 and 2017 surveys. Cross section sites were chosen along the 8 km river where there was a clear change in channel geomorphology identified by a walk-over reconnaissance of the catchment in 2016. A total of 22 sites for cross section surveys were chosen along St John's Beck. Cross section 1 was located near the St John's Beck gauging station (1 km downstream from Thirlmere Reservoir), so all data collected could be discussed in relation to the flow and rainfall records (Figs. 4b, 4c, and 5). The last cross section was located near the confluence with the River Greta (7.8 km downstream). Ten of the cross section sites were located along a 1.3 km length reach where significant riverbank erosion and overbank flood sediment deposition occurred during Storm Desmond. Survey pegs were positioned at the endpoints of each cross section in 2016 and used as control points to allow resurvey in 2017. Cross section profile RTK dGPS measurements had a mean accuracy of ± 0.02 m and standard deviation of 0.06 m in the 2016 survey, and a mean accuracy of ± 0.03 m and standard deviation of 0.03 m in the 2017 survey. Bankfull channel cross-sectional area was calculated at each cross section and changes in channel bankfull capacity ($m^2\,yr^{-1}$) were calculated by differencing the data collected over the survey periods. Thalweg long profile was surveyed using the RTK dGPS. Average profile point spacing was 8 m (mean accuracy of ± 0.02 m and standard deviation of 0.01 m) in the 2016 survey and 12 m (mean accuracy of ± 0.03 m and standard deviation of ± 0.01 m) in the 2017 survey.

Channel surface bed material was measured at each cross section following the pebble count method for grain size distribution (GSD) in the 2016 and 2017 field campaigns. The b-axis of 100 particles were randomly measured (particle under tip of the toe method; Wolman, 1954) along the width of each cross section. The median diameter grain size (D_{50}) and the 90th percentile (D_{90}) were calculated and used to understand system response and sediment transfer following the event.

4.1.2. Bedload transport

Bedload sediment transport during Storm Desmond was estimated using the Bedload Assessment for Gravel-bed Streams (BAGS) software (Pitlick et al., 2009) applying a surface-based bedload transport equation (Wilcock and Crowe, 2003). The input parameters were: the GSD of the channel bed surface, cross-sectional data including floodplains, cross section averaged bed elevation slope, flow discharge in the form of a flow exceedance curve for the event, and Manning's 'n' values for a clean winding channel (0.04) and short grass floodplains (0.03) estimated from Chow (1959). Sensitivity to Manning's 'n' values was assessed using Chow (1959) minimum and maximum values for the channel and floodplains. Morphological change between cross sections was calculated by subtracting the downstream cross section bedload transport rate from the upstream value to identify net erosion and deposition reaches.

Historical bedload sediment transport rates were also estimated using the BAGS model (i) as an average daily transport rate for the long-term daily discharge record 1935-2015, and (ii) for the top five discharge events in the long term (15 min interval) flow record. Whilst we assume that the cross-sectional profiles and grain size distribution are the same as the post-Desmond channel, this analysis allows us to assess the importance of the Storm Desmond event on sediment transport rates in relation to the longer term system history.

4.2. Geomorphic impacts of the Storm Desmond event: sediment budget analysis

A sediment budget framework was used to quantify the geomorphic impacts of the Storm Desmond event and identify the dominant stores of sediment along St John's Beck. Sediment budgets focus on quantifying the erosion, deposition and transfer of sediment through a channel or reach over an event or time period (Reid and Dunne, 1996; Brewer and Passmore, 2002; Fuller et al., 2003). Sediment budgets represent the conservation of mass and can be summarised as (Slaymaker, 2003):

$$O_S = I_s + \Delta S_s \quad (1)$$

where O_s is the sediment output (yield) of the reach, I_s is input of sediment from dynamic sediment sources, and S_s is sediment stored on floodplains, channels etc. This framework is useful to understand local sediment continuity in response to a particular event and indicate whether a system is balanced (Reid and Dunne, 2003). The main geomorphic depositional (S_s) and erosional (I_s) features identified after Storm Desmond along St John's Beck were: floodplain sediment deposits, in-channel bars, floodplain scour, channel bed scour and riverbank erosion (Fig. 3). Floodplain scour is differentiated from bank erosion as it is associated with the stripping of the floodplain surface (vegetation) and removal of large blocks of sediment (Nanson, 1986); whereas bank erosion is defined as the removal of sediment from the bank by hydraulic action or through mass failure (Odgaard, 1987; Knighton, 1998). The volume and sediment size distribution of erosional and depositional components were measured using the RTK dGPS, and pebble count technique (Wolman, 1954) and their spatial extent was validated using the pre- and post-event aerial photographs. Channel bed scour was active during the event, however, it was not directly measured as no cross sections were monumented prior to Storm Desmond. During flood events some reaches can experience scour whilst other reaches aggrade (Reid and Dunne, 1996). The location of channel bed scour was assumed to occur where riverbank erosion or floodplain scour was observed after Storm Desmond; this was quantified using the post-event air photo and field data in GIS. The depth of channel bed scour was estimated according to Carling's (1987) scour-depth relation for gravel bed rivers:

$$d_s = 0.043Q^{0.27} \quad (2)$$

where d_s is depth of scour (m) and Q is the event peak discharge (m^3 s^{-1}).

Volumes of sediment eroded and deposited for each geomorphic component were converted to sediment mass using local values of coarse sediment bulk density of 1860 ± 17 kg m^3 derived from the mean bulk density of 30 measured samples from the channel bed and floodplain sediment deposits.

Sediment input and output of St John's Beck during the event was estimated by converting the BAGS estimated event bedload sediment transport rates into (cross section 1, 1 km downstream) and out of St John's Beck (cross section 22, 7.8 km downstream) into the event sediment yield.

Error in sediment budgets represents a combination of survey measurements and calculations, so standard methods of error analysis are difficult to apply. Often, sediment budget error is calculated as an unmeasured residual by subtracting the erosion and deposition components (Kondolf and Matthews, 1991; Reid and Dunne, 2003). As a result, sediment budgets may balance only because errors are hidden in the residual terms (Kondolf and Matthews, 1991). To avoid misrepresentation of the sediment balance, in this study the standard error was calculated for each measurement technique for each geomorphic component. The standard errors were summed and then converted to a percentage before being converted to mass (t) for each component. For example, floodplain deposit mass error represents a combination of errors from the RTK dGPS, depth of deposit, and bulk density error measurements. The standard error from these measurements was calculated and then summed to calculate the total error percentage before being converted to the mass error (t).

4.3. Factors controlling geomorphic change

4.3.1. Lateral channel confinement ratio

Channel confinement describes the extent to which topography, such as hillslopes, river terraces and artificial structures, limit the lateral mobility of a river channel (Nagel et al., 2014). Lateral channel confinement ratio (C) was calculated as:

$$C = \frac{w_f}{w_c} \quad (3)$$

where w_f is the floodplain width and w_c is the active channel width. Floodplain width (pre- and post-Storm Desmond) is defined as the horizontal distance from the top of the channel bank to the base of the hillslope (Gellis et al., 2017); this is determined using the 2009-2011 and 2016 aerial photographs, the 5 m resolution DEM and the 2016 field data. The active channel width was measured (1) prior to Storm Desmond using the 2009-2011 aerial photographs, and (2) after Storm Desmond using the RTK dGPS channel cross section measurements and May 2016 aerial photographs. Channel and floodplain width were measured at the 22 cross section sites.

Hall et al. (2007) documented that confined channels have a confinement ratio of ≤3.8 and unconfined channels a ratio of >3.8. Channel confinement can influence the potential for sediment erosion and deposition; for example, Thompson and Croke (2013) found that in a high magnitude flood event in the Lockyer Valley, Australia, erosion was concentrated in the confined reaches, and deposition was concentrated in unconfined reaches with floodplains acting as a major store of sediment. Such behaviour may be affected by the presence of structures such as levees or roads, which are present along St John's Beck. Three types of confinement were identified along St John's Beck: (1) natural confinement, defined as the channel confinement by the natural valley bottom topography; (2) artificial confinement, where reaches of the channel have been modified through reinforced riverbanks, the presence of walls, levees, or road embankments that prevent the channel from migrating laterally; and (3) the post-Storm Desmond confinement taking into consideration the active channel width following the extreme event.

4.3.2. Stream power and shear stress

At the reach scale average shear stress, Eq. (4) (Du Boys, 1879), critical shear stress, Eq. (5) (Gordon et al., 1992), unit stream power, Eq. (6) (Bagnold, 1966) and critical unit stream power Eq. (7) (Bagnold, 1966; Williams, 1983; Petit et al., 2005) were calculated for the Storm Desmond flood to understand the potential magnitude of sediment transport rates and geomorphic impacts observed during the event using the one-dimensional uniform flow approximations:

$$\tau = \rho g d S \qquad (4)$$

$$\tau_c = 0.97 D_i \qquad (5)$$

$$\omega = \frac{\rho g Q S}{w} \qquad (6)$$

$$\omega_c = 0.079 D_i^{1.3} \qquad (7)$$

where τ is the reach averaged shear stress (N m^{-2}), ρ is the density of water (kg m^{-3}), *g* is the acceleration of gravity (m s^{-2}), *S* is channel bed slope (m m^{-1}) and *d* is the maximum water depth during the event (m). τ_c is the critical shear stress (N m^{-2}) and D_i is the grain size (mm). Here we use the channel D_{50} and D_{90}. ω is the unit stream power (W m^{-2}), Q corresponds to the peak discharge (m^3 s^{-1}) during Storm Desmond and w (m) is the bankfull width during the flood. ω_c is the critical unit stream power (W m^{-2}) for particle motion based on Williams' (1983) relation for gravel transport in rivers with grain sizes between 10-1500 mm. Calculations were applied at the cross section locations and the critical shear stress ($\tau > \tau_c$) and critical stream power ($\omega > \omega_c$) entrainment thresholds estimated to understand the potential for sediment mobility during the event. Shear stress and stream power calculations were also calculated using the June 2017 survey data (bankfull cross section profiles, grain size data, and mean daily discharge (0.085 m^3 s^{-1}) to quantify variation in shear stress and stream power during non-overbank flows.

5. Results

5.1. Geomorphic response to the Storm Desmond event

Storm Desmond flood impacts along St John's Beck were concentrated in the channel and on the surrounding floodplains. The spatial distributions of both erosional and depositional impacts of Storm Desmond are shown in Fig. 6a. Generally, erosion and deposition impacts were observed in spatially similar locations, for example, where bank erosion or scour occurred overbank deposition was observed. Significant erosion and deposition impacts were observed 1.7–3.6 km downstream of Thirlmere Reservoir (Fig. 6b). Geomorphic impacts were less pronounced 3.6-8 km downstream of Thirlmere Reservoir; impacts here were often concentrated locally at meander bends (e.g., as seen at 5.2 km downstream from Thirlmere Reservoir, cross section 18). Figure 6b shows a detailed map of the reach where significant geomorphic impacts (1.7–3.6 km downstream) were observed after Storm Desmond. Overbank floodplain deposits and channel bars measured 2.1–2.5 km downstream (between cross sections 7 to 10) occur where the channel is laterally unconfined. The channel in this reach (2.1-2.5 km downstream) was identified as aggradational (low channel capacity, channel bed nearly level with banks) in a reconnaissance survey (approach after Thorne, 1998) of the site prior to the flood. Bank erosion and scour was concentrated on the artificially-confined reach 2.5-3 km downstream (cross sections 10 to 13). Local lateral riverbank recession exceeded 12 m and caused the destruction of flood protection levees 2.7 km downstream of Thirlmere Reservoir (see cross section 11 Fig. 6b). Material eroded at cross section 11 was subsequently deposited on the floodplains downstream.

The dominant geomorphic features surveyed after the event were overbank floodplain sediment deposits. Floodplain sediment deposits located 1.8 km downstream (near cross section 5) were sourced from a tributary and not from St John's Beck. The tributary sediment did not enter St John's Beck due to a wall and sediment trapping structure, therefore, the mass of sediment measured here (300 t) is excluded from the sediment budget analysis. A total of 105 floodplain deposits were identified from St John's Beck, equating to a sediment mass of 4700 ± 300 t. Flood sediment deposits were generally composed of a single layer of sediment with a mean deposit depth 0.09 m ± a standard deviation of 0.07 m; the maximum flood deposit depth measured was 0.3 m located

2.7 km downstream of Thirlmere Reservoir. The mean grain size of sediment deposit D_{50} was 32 mm and D_{90} was 90 mm. The 10 largest clasts from the deposits had a mean grain size of 147 mm ± a standard deviation of 12.5 mm. Flood deposit grain size decreased with distance from the channel. The farthest flood deposit from the channel bank (70 m distance) had a D_{50} of 22 mm and D_{90} of 63 mm. The proximal flood deposits (2 m distance from the channel) had a mean D_{50} of 39 mm ± a 17 mm standard deviation and D_{90} of 111 mm ± a standard deviation of 35 mm.

Table 2 shows the variation in grain size between the flood sediment deposits and the channel bed sediments. Channel bed sediment D_{50} is greater than the floodplain sediment deposits, however, this pattern is reversed for sediment D_{90}. Floodplain sediment deposits are composed of material from the channel bed and from eroded features (such as artificial levees and stone walls), which generally have coarser grain sizes that could account for this variation.

		Floodplain Sediment Deposits	**Channel Bed Sediments (2016 Survey)**	**Channel Bed Sediments (2017 Survey)**
	Max	64	77	90
d_{50}	Mean	32	49	53
	SD	13	14	18
	Max	181	90	294
d_{90}	Mean	90	53	122
	SD	37	17	35

Table 2 Grain size (mm) of floodplain deposits and channel bed sediments in the May 2016 and June 2017 survey.

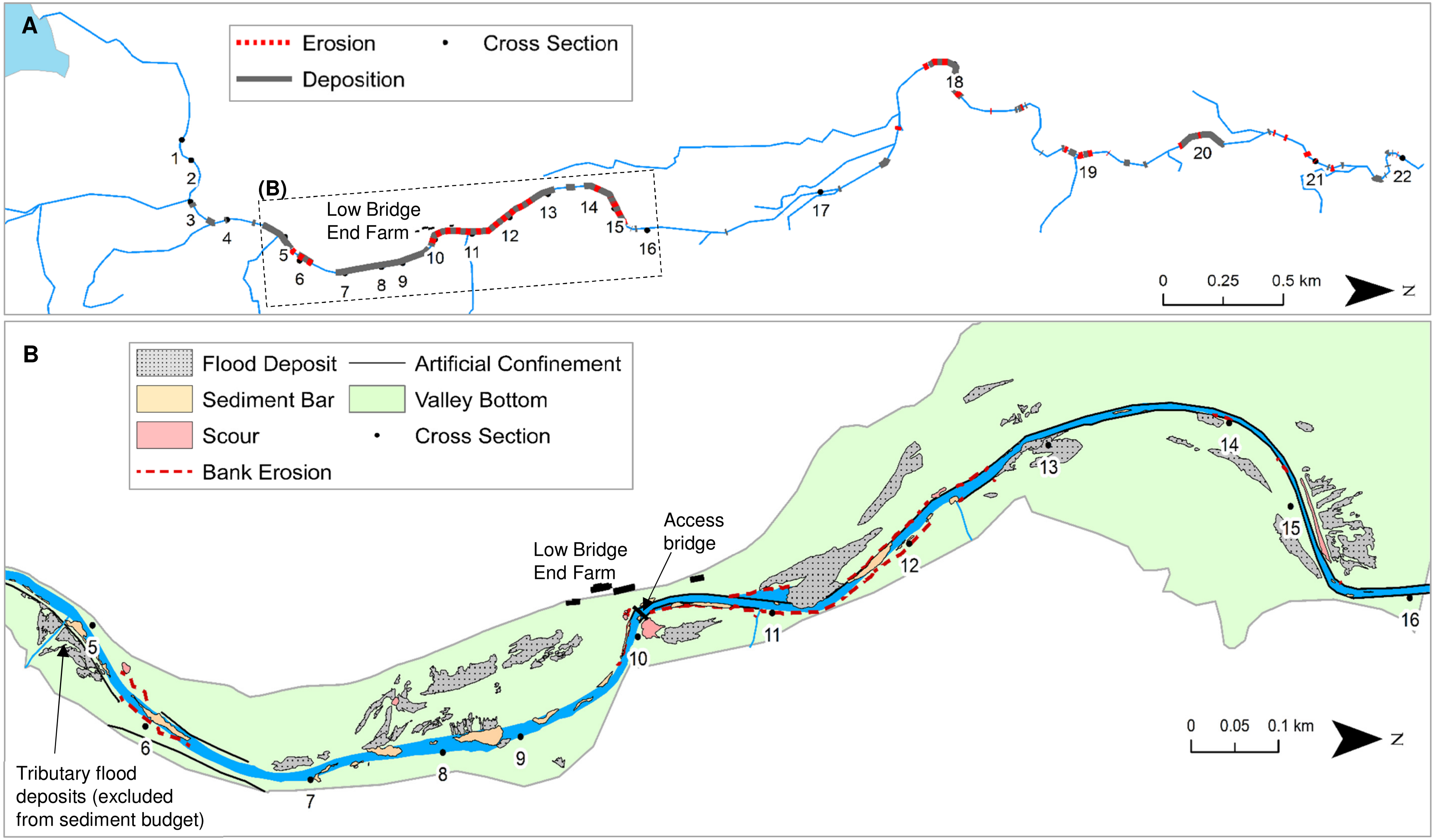

Fig. 6. Geomorphic impacts of the Storm Desmond flood event along St John's Beck, flow direction North. (A) Location of erosion and deposition impacts along St John's Beck. (B) Detailed geomorphic map showing an example reach (1.7-3.6 km downstream of Thirlmere Reservoir) with erosion and deposition impacts.

Riverbank erosion and floodplain scour were the main processes accounting for a loss of sediment during Storm Desmond. Based on the field data collected, 2300 ± 270 t of sediment was eroded from the riverbanks. Floodplain scour contributed to the removal of 1300 ± 50 t of sediment during the event, 40% of sediment removed through scour was over the reach (2.2-3.6 km downstream) where significant sediment deposition was observed. Local scour of 350 ± 13 t undermined and destroyed the access bridge to Low Bridge End Farm (see cross-section 10, 2.5 km downstream of Thirlmere Reservoir, Fig. 6). The depth of channel bed scour was estimated at 0.13 m according to Carling's (1987) scour depth equation, and this equated to a mass of 2900 ± 470 t.

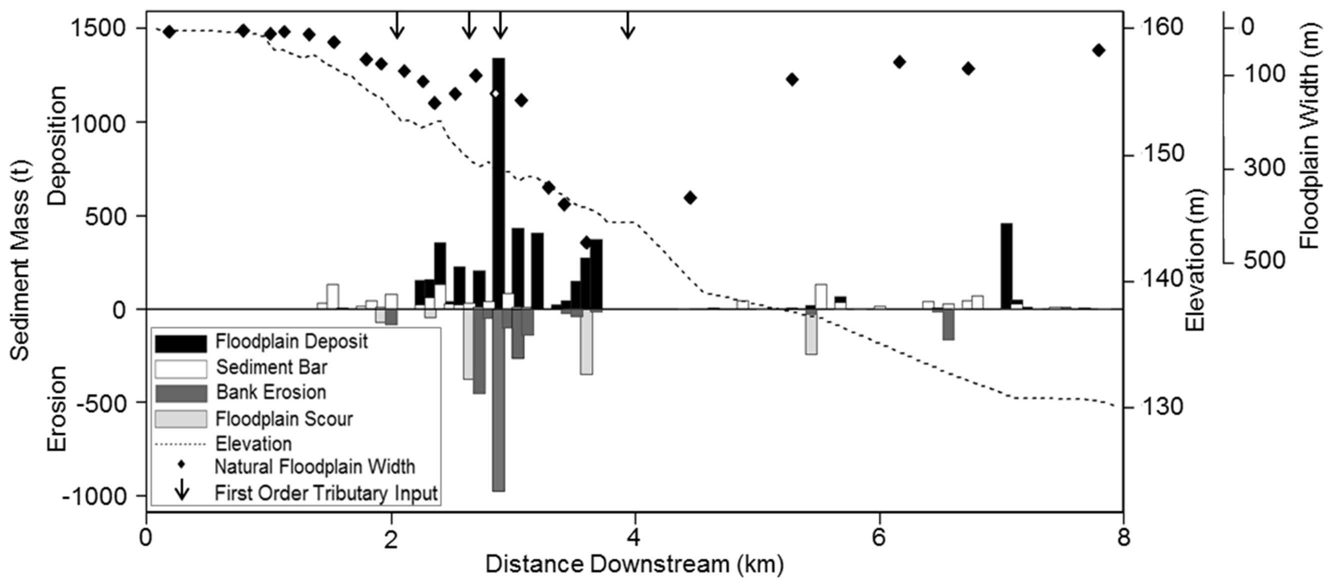

Fig. 7. Total mass (t) of sediment eroded and deposited along St John's Beck during Storm Desmond, plotted alongside the natural floodplain width and riverbed longitudinal profile.

Figure 7 displays the total mass of sediment eroded and deposited along St John's Beck during Storm Desmond. The greatest mass of sediment eroded and deposited occurs from 1.7 to 3.6 km downstream where the floodplain width increases from 7 to 450 m and channel slope steepens from 0.001 (0 to 1.7 km downstream) to 0.005 (1.7 to 3.6 km downstream). Erosion features were often balanced by sediment deposition nearby. For example, the largest mass of sediment deposited on floodplains (1340 t) correlates with the area of greatest erosion (980 t) 2.9 km downstream of Thirlmere Reservoir, where a levee was destroyed and the riverbank receded by 12 m resulting in sediment deposition over an area of 3470 m^2. Erosion and deposition impacts are less pronounced 5.2-7.8 km downstream, where the mean floodplain valley width is 77 m ± a standard deviation of 26 m, and the mean channel slope is 0.003. Erosion and deposition impacts at 5.2-7.8 km downstream were mainly concentrated on meander bends. Floodplain scour (Fig. 3c) and sediment deposition was observed on the inside of a meander bend 5.2 km downstream where overbank flows were permitted during Storm Desmond. Local bank erosion and overbank sediment deposition was observed on bends 6.8 and 7.3 km downstream.

Tree debris were observed surrounding St John's Beck following Storm Desmond. Tree debris did not cause a blockage around the access bridge to Low Bridge End Farm. However, tree debris were observed in the channel near cross section 10 (2.5 km downstream) (see Fig. 3b). The limited occurrence of woody debris in the channel inhibits the formation of log jams and only has local impacts on sedimentation.

5.2. Estimates of bedload sediment transport rate

The mean event bedload sediment transport rate for the 22 cross sections was 160 t ± a standard error of 60 t. Sediment transport rates fluctuate downstream with clear reaches of low and high sediment transfer (Fig. 8a). For example, 1.5-2 km downstream of Thirlmere Reservoir high sediment transport rates during the event (range = 220-500 t) are estimated; these are attributed to a local increase in channel slope. The maximum estimated transport rate during the event was 1200 t at 2.5 km downstream of Thirlmere Reservoir where the channel widens and local slope increases (slope 0.01) downstream of a ford, near the access bridge to Low Bridge End Farm that was destroyed during the event (Fig. 3f). The sediment input into St John's Beck during the event is estimated at 7 t (1 km downstream of Thirlmere Reservoir, cross section 1) and the sediment output (7.8 km downstream of Thirlmere reservoir, cross section 22), during the event is estimated as 370 t.

Zones of erosion and deposition along St John's Beck have been identified by differencing sediment transport rates between the surveyed cross sections (Fig. 8b). A total of 10 deposition and 11 erosion zones are defined. The zone of greatest erosion and deposition is located from 1.8 to 4 km downstream from Thirlmere Reservoir (Fig. 8b), which corresponds closely with field measurements of erosion and deposition during the event (Fig. 6).

The mean daily bedload sediment transport rate (calculated as the mean transport rate from the 22 cross sections using the 1935–2015 discharge record), is 0.05 t day^{-1} with a standard deviation of 0.09 t day^{-1}. The estimated annual bedload sediment input is estimated at 0.5 t yr^{-1} (at cross section 1) and the bedload sediment yield (at cross section 22) is 38 t yr^{-1} for St John's Beck long term discharge record. The bedload sediment output during Storm Desmond (370 t) exceeds the annual value by a factor of 9. Table 3 displays the bedload sediment transport estimates for the top five discharge events in the St John's Beck 15 min interval flow record. The Storm Desmond event produced the highest bedload sediment transport rates in the flow record, nearly double the second highest flood event in 2009.

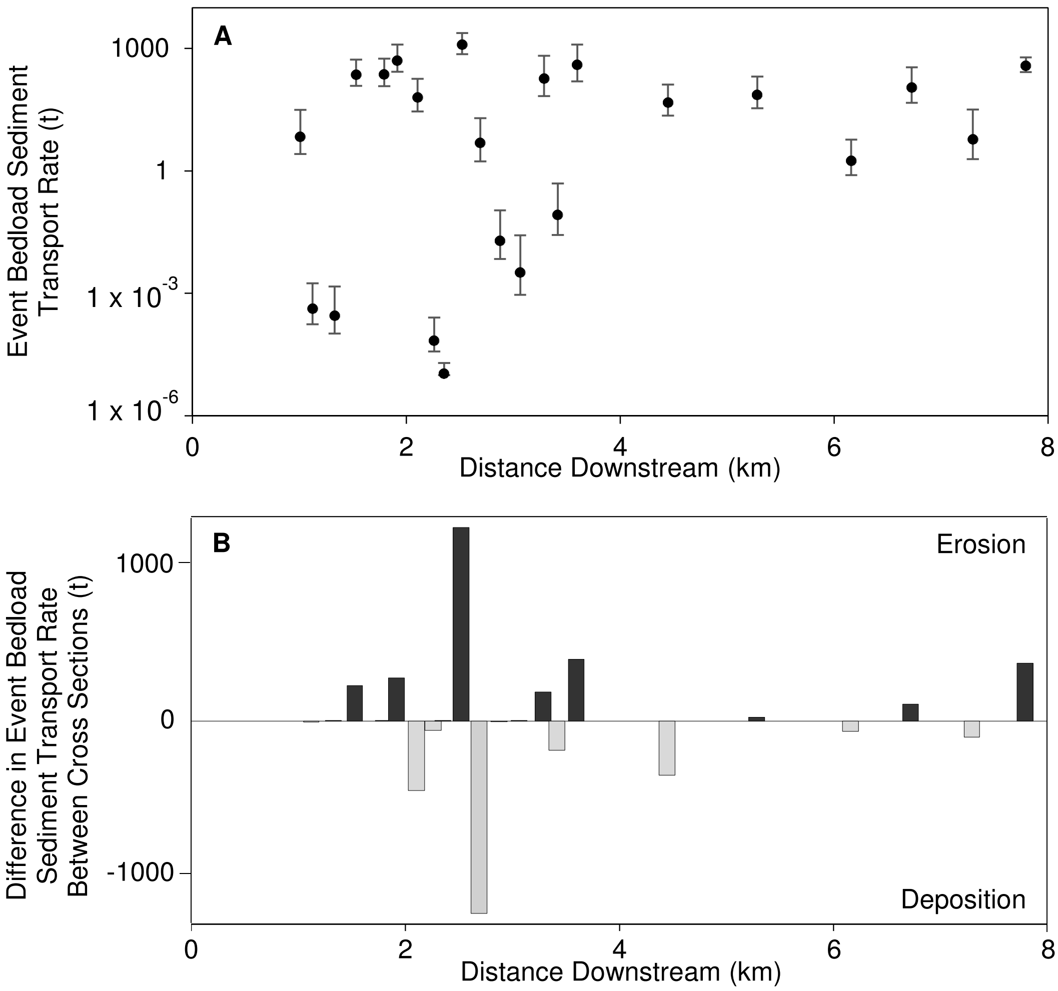

Fig. 8. Bedload sediment transport estimates along St John's Beck during Storm Desmond. (A) Storm Desmond event bedload sediment transport rates. Error bars plotted represent sensitivity to the maximum and minimum Manning's 'n' values. (B) Zones of sediment erosion and deposition downstream, calculated as the difference between sediment transport rates between cross section survey locations.

			Event Bedload Sediment Transport Rate (t)			
Date of Event	**Estimated Event Peak Discharge (m^3 s^{-1})**	**Event Rainfall Total (mm)**	**Mean**	**Std. Dev.**	**Max**	**Event Sediment Yield**
4/12/2015 - 6/12/2015	75.4	405.0	157	283	1229	370
17/12/2009 - 20/11/2009	59.8	400.0	91	166	700	210
7/01/2005 - 8/01/2005	47.7	180.0	30	55	188	70
31/01/1995 - 01/02/1995	39.0	-	25	45	151	54
21/12/1985 - 22/12/1985	36.6	-	21	41	142	32

Table 3 Bedload sediment transport estimates for the top five discharge events from the 15 min interval flow series data for St John's Beck. The event bedload transport rates are calculated as the mean transport rate from the 22 cross sections, and the event sediment yield is calculated at cross section 22.

5.3. Controlling factors that influenced geomorphic change across the reach

5.3.1. Channel Confinement Index

St John's Beck displays different degrees of lateral confinement downstream (Fig. 9). The natural channel confinement pattern shows that the channel becomes gradually unconfined downstream (Fig. 9). For example, in the upstream reach (0 to 1.8 km downstream of Thirlmere Reservoir) the channel is topographically confined (confinement ratios range from 0.1 to 0.6) and from 4.4 to 8 km downstream the channel is topographically unconfined (confinement ratios range from 5 to 65). The channel has been artificially confined from 1.8 to 4.4 km downstream by flood protection levees, reinforced banks and walls that restrict lateral channel movement. The mean natural floodplain width has been reduced by 90% due to the presence of artificial structures along the artificially confined reach 1.8 to 4.4 km downstream. During Storm Desmond, many of the artificially-reinforced banks and flood protection levees were scoured or eroded increasing the active channel width and allowing channel-floodplain interactions (Fig. 9). After Storm Desmond the mean confinement ratio increased from 0.95 to 17 along the artificially confined reach (1.8 to 4.4 km downstream), indicating the system reverted to a natural floodplain-channel width relationship (Fig. 9).

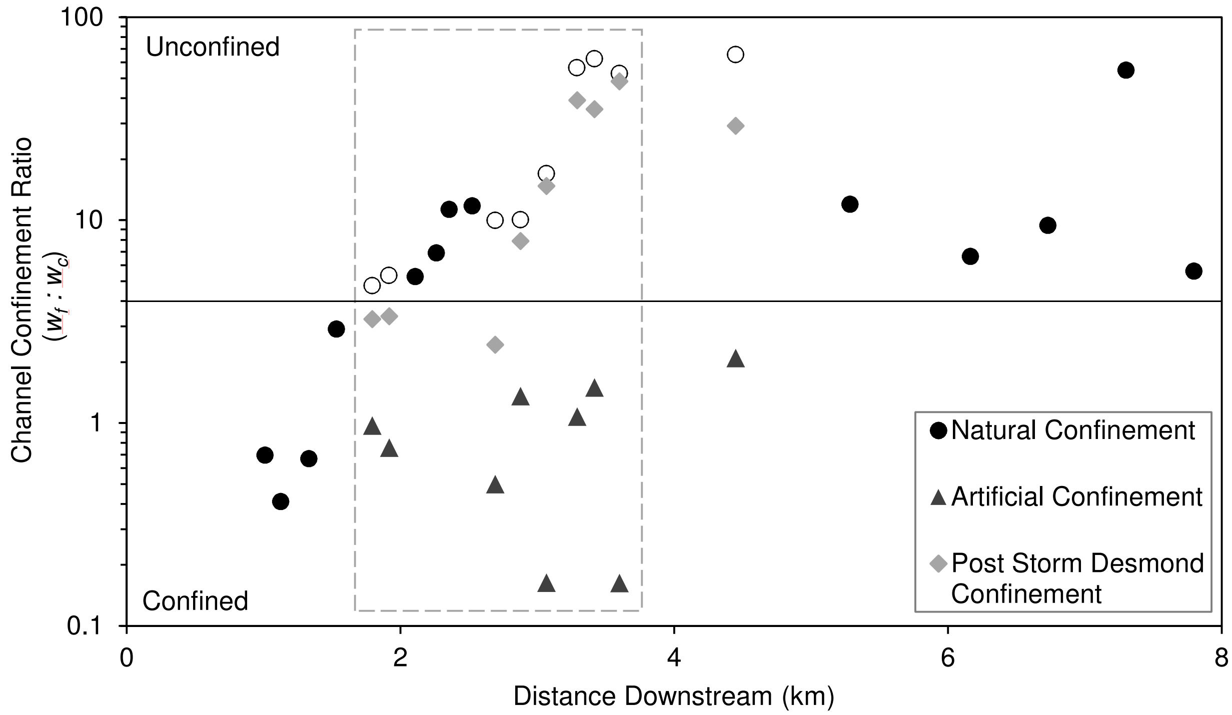

Fig. 9 Natural, artificial and post Storm Desmond lateral channel confinement ratios along St John's Beck. Hollow circles indicate the natural system if the channel was not artificially confined. The dashed box indicates the area where significant sediment erosion and deposition was observed during Storm Desmond. Continuous line indicates the confined and unconfined threshold.

5.3.2. Shear stress and stream power

Shear stress and stream power are used to understand the energy expenditure for erosion and sediment entrainment during the event (Fig. 10). The shear stress values estimated for Storm Desmond are shown in Fig. 10a. The shear stress values estimated should be regarded as minimum values because they assume shear stress is the same on the channel and floodplain and the equations assume steady uniform flow, which was unlikely during the event. The mean shear stress value is 149 N m^2 with a standard deviation of 78 N m^2. The peak shear stress value (426 N m^2) was estimated 2.7 km downstream of Thirlmere Reservoir; near where the access bridge was destroyed and mass overbank coarse sediment deposition occurred. The minimum shear stress values are estimated 1.1 to 1.3 km downstream (30-60 N m^2) where local slope is 0.001. The mean shear stress value exceeded the mean critical entrainment thresholds for particle D_{50} (48 ± a standard deviation of 14 N m^2) and D_{90} (124 ± a standard deviation of 30 N m^2) (Fig. 10a), suggesting full mobility of the GSD during the event. The mean shear stress value estimated using the 2017 survey data (62 N m^2 with a standard deviation of 40 N m^2) does not exceed the threshold for mean particle D_{90} (114 N m^2) entrainment and only exceeds 60% of the cross section particle D_{50} entrainment threshold during bankfull flow conditions.

The unit stream power values estimated along St John's Beck using the peak Storm Desmond discharge value range from 25 to 354 W m^{-2}, with a mean of 230 W m^{-2} and a standard deviation of 132 W m^{-2} (Fig. 10b). The values are within the range of stream power values documented for those causing erosion during flood events and sediment transport (Baker and Costa, 1987; Magilligan, 1992; Fuller, 2008; Marchi et al., 2016). A value of 300 W m^{-2} is commonly referred to as a threshold for producing floodplain erosion (Baker and Costa, 1987; Magilligan, 1992; Fuller, 2008). Significant erosion and scour was observed 2.5 km downstream where an access bridge was destroyed and where stream power was estimated at 420 W m^{-2}. The mean unit stream power estimate (230 W m^{-2}) exceeds the critical unit stream power value for particle D_{50} (13 W m^{-2}) and D_{90} (54 W m^{-2}) entrainment, suggesting mobilisation of the coarsest grains. The mean unit stream power, estimated using the 2017 data and mean daily discharge, is 0.26 W m^{-2} ± a standard deviation of 0.12 W m^{-2}; this value does not exceed the critical stream power threshold for channel bed particle D_{50} and D_{90} entrainment.

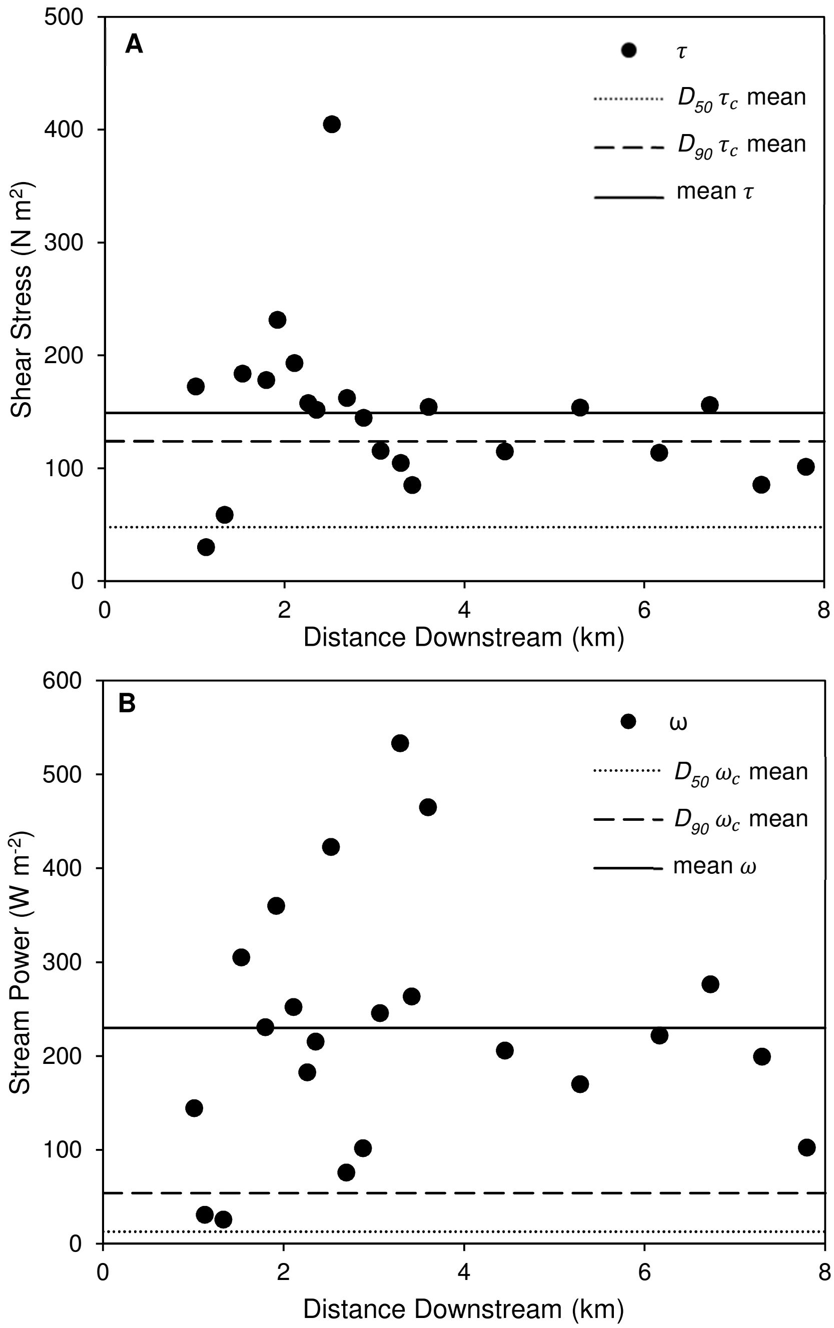

Fig. 10. Variations in reach averaged shear stress (A) and stream power (B) estimated at the cross section sites for Storm Desmond along St John's Beck.

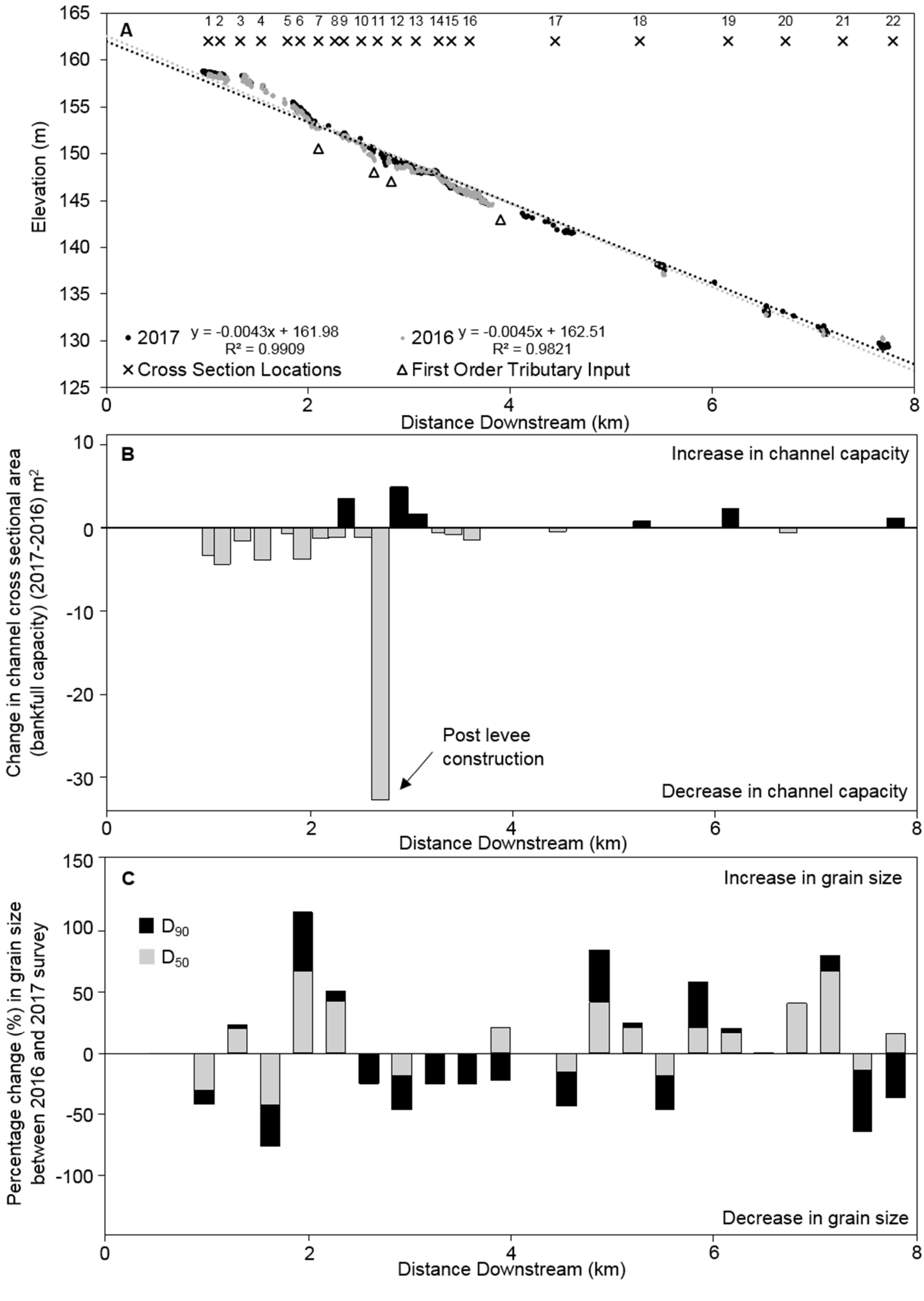

Fig. 11. Changes in St John's Beck channel long profile, bankfull capacity and grain size between the 2016 and 2017 surveys. (A) Change in bed elevation (long profile), labelled with cross section and first order tributary

locations. (B) Change in channel bankfull cross section area. (C) Percentage change in channel bed D_{50} and D_{90} grain size.

5.4. System resurvey in 2017

Resurveys of St John's Beck longitudinal profile, cross section profiles and grain size in 2017 provide an indication of how the system is recovering 1.5 yr after the extreme flood event (Fig. 11). There were no significant changes in the mean channel bed slope between the 2016 and 2017 survey, however, there were local changes where there is an increase or decrease in bed elevation height (Fig. 11a). Local changes in channel bed elevation result in changes in bankfull channel capacity (Fig. 11b). For example, at a distance of 1 to 2.4 km from Thirlmere Reservoir there is a general increase in bed elevation suggesting the deposition of sediment; a pattern further evidenced by a decrease in channel capacity. Overall a decrease in bankfull channel cross-sectional area was observed (at 15 cross sections) 1.5 yr after Storm Desmond. Thirteen of these cross-sections are located 1 to 2.7 km downstream from Thirlmere Reservoir (Fig. 11b). The largest change and reduction in channel capacity (2.7 km downstream of Thirlmere Reservoir, cross section 11) was 32.8 ± 0.03 m^2 caused by the rebuilding of flood protection levees that reduced channel width to its pre-Storm Desmond size. A total of seven cross-sections displayed either no change or an increase in cross-sectional area and channel capacity. Cross-section 9, 2.4 km downstream from Thirlmere Reservoir, shows an increase in channel capacity associated with anthropogenic removal of sediment from the channel bed after the flood event. The percentage change in grain size between the 2016 and 2017 surveys illustrates a general coarsening of bed D_{50} and fining of D_{90} downstream post Storm Desmond (Fig. 11c).

6. Discussion

6.1. Geomorphic impacts of the extreme flood event along the upland sediment cascade

The 2015 Storm Desmond event constitutes the largest recorded event in the available long term flow and rainfall records for the St John's Beck catchment (Fig. 5). The results presented here illustrate the geomorphic work of the flood in terms of sediment erosion and storage along the upper floodplain transfer zone of the USC. The main impacts were associated with erosion of river channel banks and floodplain scour allied with extensive sediment deposition on the floodplains. The summary sediment budget (Fig. 12) shows erosion (6500 ± 710 t) was generally balanced by deposition (6300 ± 570 t) along the upper floodplain zone. Less than 6% of the total sediment eroded during the event was transferred out of the reach. Hence, the upper floodplain zone acted as a significant sink for locally-eroded sediment during the extreme event.

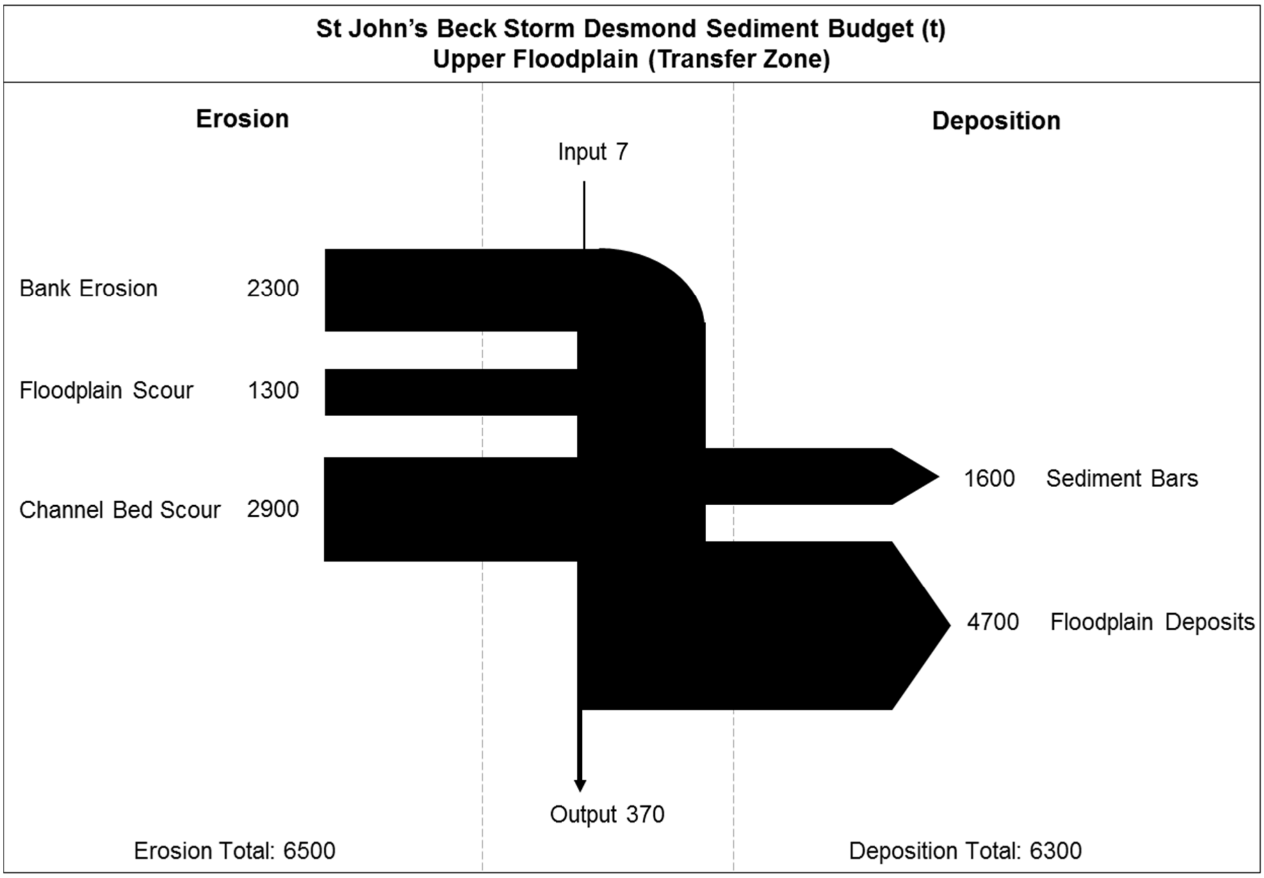

Fig. 12. Storm Desmond (2015) upper floodplain valley system (transfer zone) mass sediment budget (t) for St John's Beck (effective catchment area 12 km^2).

The geomorphic impacts of Storm Desmond were influenced by the physical characteristics of the upper floodplain transfer zone. Unlike steep headwater catchments dominated by slope-channel linkages and hillslope processes (Harvey, 2001), geomorphic impacts of the event along St John's Beck were controlled by floodplain-channel interactions. Tributaries were only a minor source of sediment as these were disconnected from the channel by sediment trapping structures and therefore are not reported in the sediment budget in Fig. 12. Sediment was sourced from transient stores, i.e., channel bars) and through erosion of the channel bed and banks and stored in channel bars and on the surrounding floodplains (Fig. 6).

Valley confinement (natural and artificial) controlled the spatial positioning of erosional and depositional storm impacts along St John's Beck (Fig. 9). In the upstream reaches (0 to 1.8 km downstream) the channel was confined by the natural valley topography and geomorphic impacts were comprised of local erosion or sediment bar deposition. Where the natural floodplain valley width increases from 3 to 160 m (1.8 km downstream) and there is an associated decrease in channel slope, rapid floodplain sediment deposition occurred (Fig. 7). In contrast, artificially confined reaches (2.7 to 3.6 km downstream) were associated with bank erosion or scour due to local increases in channel bed slope. Major riverbank erosion was observed along an artificially confined reach 2.7 km downstream of Thirlmere Reservoir; here riverbanks were eroded until the channel became unconfined (Fig. 9) with extensive floodplain sedimentation. Similar effects have been observed by Magilligan (1985), Nanson (1986), Butler and Malanson (1993), Lecce (1997), Fuller (2007, 2008), who all identified a concentration of erosion on constricted reaches. The transition between confined and unconfined reaches therefore plays an important role in controlling the spatial pattern of erosion and deposition impacts of these events.

6.3. Sediment continuity through the upland sediment cascade

The sediment continuity concept focuses on the principle of mass conservation of sediment within a system (Slaymaker, 2003; Hinderer, 2012). The USC sediment continuity has been described as a 'jerky conveyor belt', where sediment can spend a longer time in storage than in transfer (Ferguson, 1981; Walling, 1983; Newson, 1997; Otto et al., 2009). This study has highlighted that sediment continuity is disrupted or 'discontinuous' at the event scale due to storage. Less than 6% of sediment eroded during Storm Desmond was transported out of St John's Beck (Fig. 12). Elsewhere, sediment budget studies have shown similar inefficiencies in sediment transfer, often referring to this as the 'sediment delivery problem' (Trimble, 1983; Walling, 1983; Phillips, 1991; McLean et al., 1999; Fryirs, 2013). For example, in the Coon Creek Basin, USA, less than 7% of sediment left the basin between 1853 and 1977 (Trimble, 1983). In the River Coquet, UK, annual sediment budget within-reach sediment transfer was identified but there was minimal net export of sediment downstream (Fuller et al., 2002). In three UK upland catchments, Warburton (2010) demonstrated sediment transfer is inefficient in the production zone by comparing sediment budgets on an annual, landslide event and flood event timescale. Despite variations in catchment area and the timescale of enquiry, these examples demonstrate there is attenuation of sediment downstream due to sediment storage. This study highlights the importance of the floodplain as a major store of sediment at the event scale causing sediment attenuation at the channel outlet.

The Storm Desmond event sediment yields were higher than estimated sediment yields for previous flood events along St John's Beck (Table 3), indicating the event was significant in generating and transporting large quantities of sediment downstream. The estimated mean shear stress and unit stream power values for Storm Desmond exceeded the thresholds for particle entrainment, suggesting sediment on the channel bed was mobilised and transported during the event (Fig. 10). Despite this, the event sediment yield is lower than the total quantity of sediment eroded. Sediment transfer during extreme events, where overbank flows are produced, is reduced on the floodplains (because of variations in roughness, slope, local topography) compared to the channel, resulting in sediment deposition (Trimble, 1983; Moore and Newson, 1986). Consequently, sediment continuity through the upper floodplain transfer zone during extreme events will ultimately be controlled by the conveyance of sediment across floodplains, and the propensity for sediment deposition during overbank flows. Future flood events may promote exchanges in sediment stores and movement of sediment downstream in pulses or waves, thereby influencing sediment yield (Nicholas et al., 1995). However, if a future similar magnitude event were to occur along St John's Beck, it is likely that the reach sediment output would again be lower than the total sediment eroded along the river corridor due to deposition on the floodplains.

Previous studies have described the potential linkages between sources and stores of sediment in terms of connectivity or disconnectivity (Hooke, 2003; Fryirs, 2013; Bracken et al., 2015). However, few of these studies have quantified the mass exchange of sediment between different landscape units during flood events (Thompson et al., 2016) and assessed their impact on sediment yield. This study is among the first to effectively quantify sediment attenuation in the upper floodplain zone of the USC during an extreme event.

6.3. System recovery

Fluvial systems can take decades (Wolman and Gerson, 1978; Sloan et al., 2001) to millennia (Lancaster and Casebeer, 2007) to recover from extreme events, with some systems never fully recovering to the pre-flood condition. The channel re-survey one year after Storm Desmond showed that 70% of cross sections had a reduced channel capacity reflecting sediment aggradation in the channel (Fig. 11). A reconnaissance survey prior to Storm Desmond identified distinct reaches of sediment aggradation in the system (in particular, 2 to 2.5 km downstream of Thirlmere Reservoir), suggesting the river is displaying characteristics similar to the pre-flood system. Long term flow regulation and upstream sediment trapping by Thirlmere Reservoir has influenced sediment continuity, implying that the sediment regime is already disturbed by the legacy of anthropogenic modification (Wohl, 2015). Phillips (1991) states that stores of sediment may develop in fluvial systems so the system can maintain sediment yields when sediment from upstream is reduced. The critical shear stress and critical stream power entrainment thresholds for channel bed particle D_{90} estimated using the 2017 survey data were not exceeded during daily flows after storm Desmond indicting coarse sediment immobility. It is likely that the finer material was transported in 2017 and deposited downstream in aggradational zones where channel dimensions change (i.e., reduction in slope, width and depth), resulting in further aggradation downstream and apparent coarsening in reaches where the fine sediment was partially mobilised. Therefore local aggradation observed could be a response to long-term system disturbance and transport-limited flows.

The most significant changes observed along St John's Beck one year after the flood were associated with anthropogenic modifications to the system through the rebuilding of flood protection levees, reinforced river banks and removal of sediment from the channel bed and floodplains (2 to 4 km downstream); these modifications took place after the 2016 field campaign. Distal floodplain deposits were located 70 m from the channel and therefore can only be remobilised during overbank flows with similar peak discharges where the critical entrainment thresholds are exceeded. Consequently, system recovery and sediment transfer depends on the conveyance capacity of the valley floodplains in addition to the stream channel capacity (Trimble, 2010). If sediment was not anthropogenically removed from the floodplains, it would have a long residence time in this store and only be remobilised during overbank extreme flows similar to Storm Desmond. Flood levees were rebuilt 2.7 km downstream to the pre-flood position, it is likely that if these levees were not restored the river would permanently occupy the post-Storm Desmond position; a natural 're-wilding' process (Fryirs and Brierley, 2016).

7. Conclusions

This paper has quantified the geomorphic response of an upper floodplain river system (transfer zone) to an extreme high magnitude flood event: Storm Desmond, 2015. The results highlight that sediment continuity along upland rivers is complex and to fully understand the response of these systems to extreme events, sediment continuity in the context of the upland sediment cascade needs to be understood (Fig. 1). Based on our results, the primary conclusions of this work are:

1. Sediment continuity through the upper floodplain transfer zone was highly disrupted during Storm Desmond, with less than 6% of the eroded sediment being transported out of the system.
2. Floodplains acted as a major sink of coarse sediment during the flood, storing 72% of the eroded sediment, although these floodplains can also be a source of sediment through scouring and erosion processes.
3. Spatial patterns of erosion and deposition were controlled by valley confinement; where the channel is naturally unconfined overbank floodplain deposits were prominent, in contrast, in artificially-confined reaches, bank erosion and scour were dominant geomorphic impacts.
4. The event exceeded critical entrainment thresholds for channel bed particle D_{50} and D_{90} transporting sediment that had aggraded in the channel. Critical entrainment thresholds were not exceeded during daily flows for all particle sizes along St John's Beck in the 2017 survey.

5. Channel capacity decreased 1.5 yr after the event and channel bed grain size had coarsened due to aggradation in the channel.

This study has quantified the importance of the upper floodplain zone in regulating sediment output during extreme events. The results suggest that rather than envisioning upper floodplain zones as effective transfer reaches they are actually major storage zones that capture flood sediments and disrupt sediment continuity downstream. The intervening valley floodplain geomorphology (confinement, slope) plays a major role in influencing the spatial location of erosion and deposition impacts.

Acknowledgements

The authors thank Graham, Sarah and William Chaplin-Bryce and their family for allowing access to St John's Beck and for valuable discussions of their experience of the Storm Desmond flood and the history of the river. A. Cartwright, G. Paxman, V. Smith and R. Smith are all thanked for their help collecting the field data at various stages. Thanks are due to the Environment Agency for supplying aerial photograph, rainfall and discharge data. Hannah M. Joyce was funded by a Natural Environmental Research Council UK Studentship Grant Number NE/L002590/1. Jeff Warburton was supported by a Natural Environmental Research Council Urgency Grant NE/P000118/1.

References

Ashbridge, D., 1995. Processes of river bank erosion and their contribution to the suspended sediment load of the River Culm, Devon. In: Foster I., Gurnell A., Webb B. (Eds.), Sediment and water quality in river catchments. John Wiley and Sons, Chichester, pp. 229-245.

Bagnold, R.A., 1966. An approach to the sediment transport problem from general physics. U.S. Geological Survey Proffessional Paper 422-I. United States Government Printing Office, Washington.

Baker, V., Costa, J., 1987. Flood power. In: Mayer L., Nash D. (Eds.), Catastrophic Flooding. Allen and Unwin, Boston pp. 1-20.

BBC, 2016. Flood-hit A591: Closure 'to cost Lake District £1m a day'. http://www.bbc.co.uk/news/uk-england-cumbria-35547704 Last Accessed: 13/10/2017

Bracken, L.J., Turnbull, L., Wainwright, J., Bogaart, P., 2015. Sediment connectivity: a framework for understanding sediment transfer at multiple scales. Earth Surface Processes and Landforms 40(2), 177-188.

Brewer, P.A., Passmore, D.G., 2002. Sediment budgeting techniques in gravel-bed rivers. Geological Society, London, Special Publications 191(1), 97-113.

Bromley, J., 2015. Thirlmere Catchment Sediment Management Plan, United Utilities, Warrington, pp. 37.

Butler, D,R., Malanson, G.P., 1993. An unusual early-winter flood and its varying geomorphic impact along a subalpine river in the Rocky Mountains. Zeitschrift fur Geomorphologie 37(2),145-155.

Burt, T., Allison, R.J., 2010. Sediment Cascades: An Integrated Approach. John Wiley and Sons, Chichester.

Caine, N., Swanson, F., 2013. Geomorphic coupling of hillslope and channel systems in two small mountain basins. In: Slaymaker O. (Ed.), Geomorphology: Critical Concepts in Geography. Routledge, Oxon, pp. 159-173.

Carling, P., 1987. Bed stability in gravel streams, with reference to stream regulation and ecology. River channels: environment and process. Blackwell Scientific Publications, Oxford, UK, 321-347.

Carling, P., 1988. The concept of dominant discharge applied to two gravel-bed streams in relation to channel stability thresholds. Earth Surface Processes and Landforms 13(4), 355-367.

CEH, 2015. North West Floods - Hydrological Update. https://www.ceh.ac.uk/news-and-media/blogs/north-west-floods-hydrological-update.

Church, M., 2002. Geomorphic thresholds in riverine landscapes. Freshwater Biology 47(4), 541-557.

Chorley, R.J., Kennedy, B.A., 1971. Physical Geography: A Systems Approach. Prentice-Hall International, London.

Chow, T.V., 1959. Open-channel Hydraulics. McGraw-Hill Inc New York.

Crozier, M.J., 2010. Landslide geomorphology: an argument for recognition, with examples from New Zealand. Geomorphology 120(1-2), 3-15.

Davies, T.R., Korup, O., 2010. Sediment cascades in active landscapes. In: Burt T., Allison R.J. (Eds.), Sediment Cascades: An Integrated Approach. John Wiley and Sons, Chichester, pp. 89-115.

Du Boys, M., 1879. The Rhone and streams with movable beds. Annals des Pontes et Chaussees 18, 141-195.

Edina Digimap, 2016. EDINA Digimap Data Collection. https://digimap.edina.ac.uk/

Environment Agency, 2006. Cumbria Floods Technical Report, Factural report on meterology, hydrology and impacts of the January 2005 flooding in Cumbria. http://www.bramptonweather.co.uk/data/CarlisleFloods2005.pdf

Ferguson, R.I., 1981. Channel forms and channel changes. In: Lewin J. (Ed.), British Rivers. George Allen and Unwin, London, pp. 90-125.

Foster, I.D., 2010. Lakes and reservoirs in the sediment cascade. In: Burt T., Allison R.J. (Eds.), Sediment Cascades: An Integrated Approach. John Wiley and Sons, Chichester, pp. 345-376.

Fryirs, K., 2013. (Dis)Connectivity in catchment sediment cascades: a fresh look at the sediment delivery problem. Earth Surface Processes and Landforms 38(1), 30-46.

Fryirs, K.A., Brierley, G.J., 2016. Assessing the geomorphic recovery potential of rivers: forecasting future trajectories of adjustment for use in management. Wiley Interdisciplinary Reviews: Water 3(5), 727-748.

Fryirs, K.A., Brierley, G.J., Preston, N.J., Kasai, M., 2007. Buffers, barriers and blankets: the (dis)connectivity of catchment-scale sediment cascades. Catena 70(1), 49-67.

Fuller, I.C., 2007. Geomorphic work during a "150-year" storm: contrasting behaviors of river channels in a New Zealand catchment. Annals of the Association of American Geographers 97(4), 665-676.

Fuller, I.C., 2008. Geomorphic impacts of a 100-year flood: Kiwitea Stream, Manawatu catchment, New Zealand. Geomorphology 98(1), 84-95.

Fuller, I., Passmore, D., Heritage, G., Large, A., Milan, D., Brewer, P., 2002. Annual sediment budgets in an unstable gravel-bed river: the River Coquet, northern England. Geological Society, London, Special Publications 191(1), 115-131.

Fuller, I.C., Large, A.R.G., Charlton, M.E., Heritage, G.L., Milan, D.J., 2003. Reach-scale sediment transfers: an evaluation of two morphological budgeting approaches. Earth Surface Processes and Landforms 28(8), 889-903.

Fuller, I.C., Riedler, R.A., Bell, R., Marden, M., Glade, T., 2016. Landslide-driven erosion and slope-channel coupling in steep, forested terrain, Ruahine Ranges, New Zealand, 1946-2011. Catena 142, 252-268.

Gellis, A.C., Myers, M.K., Noe, G.B., Hupp, C.R., Schenk, E.R., Myers, L., 2017. Storms, channel changes, and a sediment budget for an urban-suburban stream, Difficult Run, Virginia, USA. Geomorphology 278, 128-148.

Gergel, S.E., Dixon, M.D., Turner, M.G., 2002. Consequences of human-altered floods: levees, floods, and floodplain forests along the Wisconsin River. Ecological Applications 12(6), 1755-1770.

Gordon, N.D., McMahon, T.A., Finlayson, B.L., 1992. Sediment Motion, Stream Hydrology: An Introduction for Ecologists. John Wiley and Sons, Chichester, pp. 324-336.

Gurnell, A.M., 1983. Downstream channel adjustments in response to water abstraction for hydro-electric power generation from alpine glacial melt-water streams. The Geographical Journal 149(3), 342-354.

Hall, J.E., Holzer, D.M., Beechie, T.J., 2007. Predicting river floodplain and lateral channel migration for salmon habitat conservation. Journal of the American Water Resources Association 43(3), 786-797.

Harvey, A.M., 2001. Coupling between hillslopes and channels in upland fluvial systems: implications for landscape sensitivity, illustrated from the Howgill Fells, northwest England. Catena 42(2-4), 225-250.

Harvey, A.M., 2007. Differential recovery from the effects of a 100-year storm: significance of long-term hillslope–channel coupling; Howgill Fells, northwest England. Geomorphology 84(3–4), 192-208.

Herdendorf, C.E., 1982. Large lakes of the world. Journal of Great Lakes Research 8(3), pp.379-412.

Hey, R., Winterbottom, A., 1990. River engineering in National Parks: the case of the River Wharfe, UK. Regulated Rivers: Research & Management 5(1), 35-44.

Hinderer, M., 2012. From gullies to mountain belts: a review of sediment budgets at various scales. Sediment Geol. 280, 21-59.

Hooke, J., 2003. Coarse sediment connectivity in river channel systems: a conceptual framework and methodology. Geomorphology 56(1), 79-94.

Johnson, R., Warburton, J., Mills, A., 2008. Hillslope–channel sediment transfer in a slope failure event: Wet Swine Gill, Lake District, northern England. Earth Surface Processes and Landforms 33(3), 394-413.

Johnson, R.M., Warburton, J., 2002. Flooding and geomorphic impacts in a mountain torrent: Raise Beck, Central Lake District, England. Earth Surface Processes and Landforms 27(9), 945-969.

Johnson, R.M., Warburton, J., 2006. Variability in sediment supply, transfer and deposition in an upland torrent system: Iron Crag, northern England. Earth Surface Processes and Landforms 31(7), 844-861.

Knighton, D., 1998. Fluvial Forms and Processes: A New Perspective. Arnold, London.

Knox, J.C., 2006. Floodplain sedimentation in the Upper Mississippi Valley: natural versus human accelerated. Geomorphology 79(3), 286-310.

Kondolf, G.M., 1997. PROFILE: hungry water: effects of dams and gravel mining on river channels. Environmental Management 21(4), 533-551.

Kondolf, G.M., Matthews, W.V.G., 1991. Unmeasured residuals in sediment budgets - a cautionary note. Water Resour. Res. 27(9), 2483-2486.

Korup, O., 2005. Geomorphic imprint of landslides on alpine river systems, southwest New Zealand. Earth Surface Processes and Landforms 30(7), 783-800.

Korup, O., 2012. Earth's portfolio of extreme sediment transport events. Earth-Science Reviews 112(3-4), 115-125.

Krapesch, G., Hauer, C., Habersack, H., 2011. Scale orientated analysis of river width changes due to extreme flood hazards. Natural Hazards and Earth System Sciences 11(8), 2137.

Lancaster, S.T., Casebeer, N.E., 2007. Sediment storage and evacuation in headwater valleys at the transition between debris-flow and fluvial processes. Geology 35(11), 1027-1030.

Langhammer, J., 2010. Analysis of the relationship between the stream regulations and the geomorphologic effects of floods. Natural Hazards 54(1), 121-139.

Lecce, S.A., 1997. Spatial patterns of historical overbank sedimentation and floodplain evolution, Blue River, Wisconsin. Geomorphology, 18(3-4), 265-277.

Lewin, J., 1981. British Rivers. George Allen and Unwin, London.

Lewin, J., 2013. Enlightenment and the GM floodplain. Earth Surface Processes and Landforms 38(1), 17-29.

Lisenby, P.E., Croke, J., Fryirs, K.A., 2018. Geomorphic effectiveness: a linear concept in a non-linear world. Earth Surface Processes and Landforms 43(1), 4-20.

Magilligan, F.J., 1985. Historical floodplain sedimentation in the Galena River basin, Wisconsin and Illinois. Ann Assoc Am Geogr, 75(4), 583-594.

Magilligan, F.J., 1992. Thresholds and the spatial variability of flood power during extreme floods. Geomorphology 5(3-5), 373-390.

Marchi, L., Cavalli, M., Amponsah, W., Borga, M., Crema, S., 2016. Upper limits of flash flood stream power in Europe. Geomorphology 272, 68-77.

McCarthy, M., Spillane, S., Walsh, S., Kendon, M., 2016. The meteorology of the exceptional winter of 2015/2016 across the UK and Ireland. Weather 71(12), 305-313.

McDougall, D., Evans, D., 2015. The Quaternary of the Lake District Field Guide. Quaternary Research Association.

McLean, D.G., Church, M., Tassone, B., 1999. Sediment transport along lower Fraser River - 1. Measurements and hydraulic computations. Water Resour. Res. 35(8), 2533-2548.

Met Office, 2016. Flooding in Cumbria December 2015. https://www.metoffice.gov.uk/climate/uk/interesting/december2015. Last Accessed: February 2018

Milan, D.J., 2012. Geomorphic impact and system recovery following an extreme flood in an upland stream: Thinhope Burn, northern England, UK. Geomorphology 138(1), 319-328.

Milliman, J.D., Syvitski, J.P.M., 1992. Geomorphic tectonic control of sediment discharge to the ocean - the importance of small mountainous rivers. J. Geol. 100(5), 525-544.

Montgomery, D.R., Buffington, J.M., 1993. Channel classification, prediction of channel response, and assessment of channel condition. Department of Geological Sciences and Quaternary Research Centre, University of Washington, Washington.

Moore, R.J., Newson, M.D., 1986. Production, storage and output of coarse upland sediments - natural and artificial influences as revealed by research catchment studies. J. Geol. Soc. London 143, 921-926.

Nagel, D.E., Buffington, J.M., Parkes, S.L., Wenger, S., Goode, J.R., 2014. A landscape scale valley confinement algorithm: delineating unconfined valley bottoms for geomorphic, aquatic, and riparian applications. Rocky Mountain Research Station Fort Collins, US Department of Agriculture, Forest Service.

Nanson, G.C., 1986. Episodes of vertical accretion and catastrophic stripping: a model of disequilibrium flood-plain development. Geological Society of America Bulletin 97(12), 1467-1475.

Newson, M., 1997. Time, scale and change in river landscapes: the jerky conveyor belt. Landscape Research 22(1), 13-23.

Nicholas, A., Ashworth, P., Kirkby, M., Macklin, M., Murray, T., 1995. Sediment slugs: large-scale fluctuations in fluvial sediment transport rates and storage volumes. Prog. Phys. Geog. 19(4), 500-519.

Odgaard, A.J., 1987. Streambank erosion along two rivers in Iowa. Water Resour. Res. 23(7), 1225-1236.

Otto, J.C., Schrott, L., Jaboyedoff, M., Dikau, R., 2009. Quantifying sediment storage in a high alpine valley (Turtmanntal, Switzerland). Earth Surface Processes and Landforms 34(13), 1726-1742.

Petit, F., Gob, F., Houbrechts, G., Assani, A., 2005. Critical specific stream power in gravel-bed rivers. Geomorphology 69(1-4), 92-101.

Petts, G.E., 1979. Complex response of river channel morphology subsequent to reservoir construction. Prog. Phys. Geog. 3(3), 329-362.

Petts, G.E., Thoms, M.C., 1986. Channel aggradation below Chew valley lake, Somerset, UK. Catena 13(3), 305-320.

Petts, G.E., Gurnell, A.M., 2005. Dams and geomorphology: research progress and future directions. Geomorphology 71(1), 27-47.

Phillips, J.D., 1991. Fluvial sediment budgets in the North-Carolina Piedmont. Geomorphology 4(3-4), 231-241.

Pitlick, J., Cui, Y., Wilcock, P., 2009. Manual for computing bed load transport using BAGS (Bedload Assessment for Gravel-bed Streams) Software.

Prosser, I.P., Hughes, A.O., Rutherfurd, I.D., 2000. Bank erosion of an incised upland channel by subaerial processes: Tasmania, Australia. Earth Surface Processes and Landforms 25(10), 1085-1101.

Raven, E.K., Lane, S.N. and Bracken, L.J., 2010. Understanding sediment transfer and morphological change for managing upland gravel-bed rivers. Progress in Physical Geography, 34(1), x23-45.

Reid, H., 2014. Thirlmere Gravel Management. Environment Agency, Cumbria, pp. 23.

Reid, L.M., Dunne, T., 1996. Rapid evaluation of sediment budgets, 29. Catena Reiskirchen, Germany.

Reid, L.M., Dunne, T., 2003. Sediment budgets as an organizing framework in fluvial geomorphology. Tools in fluvial geomorphology, 357-380.

Righini, M., Surian, N., Wohl, E., Marchi, L., Comiti, F., Amponsah, W., Borga, M., 2017. Geomorphic response to an extreme flood in two Mediterranean rivers (northeastern Sardinia, Italy): analysis of controlling factors. Geomorphology 290, 184-199.

Roberts, N.M., Cole, S.J., Forbes, R.M., Moore, R.J., Boswell, D., 2009. Use of high-resolution NWP rainfall and river flow forecasts for advance warning of the Carlisle flood, north-west England. Meteorological Applications 16(1), 23-34.

Schumm, S.A., 1977. The Fluvial System. John Wiley and Sons, New York.

Sear, D., Wheaton, J., Neal, J., Andersen, E., Leyalnd, J., Hornby, D., Bates, P., Murdoch, A., Dearing, J., 2017. Valley and human controls on the geomorphic responses to an extreme flood, Cumbrian Floods Partnership Geomorphology Workshop Penrith, UK.

Sibley, A., 2010. Analysis of extreme rainfall and flooding in Cumbria 18–20 November 2009. Weather 65(11), 287-292.

Slaymaker, O., 1991. Mountain geomorphology: a theoretical framework for measurement programmes. Catena 18(5), 427-437.

Slaymaker, O., 2003. The sediment budget as conceptual framework and management tool, The Interactions Between Sediments and Water. Springer, pp. 71-82.

Sloan, J., Miller, J.R., Lancaster, N., 2001. Response and recovery of the Eel River, California, and its tributaries to floods in 1955, 1964, and 1997. Geomorphology 36(3), 129-154.

Smith, G., 1754. Dreadful storm in Cumberland. Gentleman's Magazine 24, 464-467.

Smith, H.G., Dragovich, D., 2008. Sediment budget analysis of slope–channel coupling and in-channel sediment storage in an upland catchment, southeastern Australia. Geomorphology 101(4), 643-654.

Stewart, L., Morris, D., Jones, D., Spencer, P., 2010. Extreme rainfall in Cumbria, November 2009-an assessment of storm rarity, BHS Third International Symposium, Managing Consequences of a Changing Global Environment, Newcastle.

Stewart, L., Vesuviano, G., Morris, D., Prosdocimi, I., 2014 The new FEH rainfall depth-duration-frequency model: results, comparisons and implications. [Speech] In: 12th British Hydrological Society National Symposium, Birmingham, UK, 2-4 Sept 2014

Strahler, A.N., 1952. Hypsometric (area-altitude) analysis of erosional topography. Geological Society of America Bulletin 63(11), 1117-1142.

Thompson, C., Croke, J., 2013. Geomorphic effects, flood power, and channel competence of a catastrophic flood in confined and unconfined reaches of the upper Lockyer valley, southeast Queensland, Australia. Geomorphology 197, 156-169.

Thompson, C.J., Fryirs, K., Croke, J., 2016. The disconnected sediment conveyor belt: patterns of longitudinal and lateral erosion and deposition during a catastrophic flood in the Lockyer Valley, South East Queensland, Australia. River Res. Appl. 32(4), 540-551.

Trimble, S.W., 1983. A sediment budget for Coon Creek Basin in the Driftless Area, Wisconsin, 1853-1977. American Journal of Science 283(5), 454-474.

Trimble, S.W., 2010. Streams, valleys and floodplains in the sediment cascade. In: Burt T., Allison R.J. (Eds.), Sediment Cascades: An Integrated Approach. John Wiley and Sons, Chichester, pp. 307-343.

van Oldenborgh, G.J., Otto, F.E., Haustein, K., Cullen, H., 2015. Climate change increases the probability of heavy rains like those of storm Desmond in the UK-an event attribution study in near-real time. Hydrology & Earth System Sciences Discussions 12(12).

Wallace, M., Atkins, J., 1997. A medium term study of the Salmonid populations in St John’s Beck and the River Glenderamackin (River Derwent, Cumbria) 1974 to 1996. Environment Agency, Cumbria.

Walling, D.E., 1983. The sediment delivery problem. Journal of Hydrology 65(1-3), 209-237.

Warburton, J., 2010. Sediment transfer in steep upland catchments (Northern England, UK): landform and sediment source coupling. In: Otto J.-C., Dikau R. (Eds.), Landform - Structure, Evolution, Process Control. Lecture Notes in Earth Sciences. Springer Berlin Heidelberg, pp. 165-183.

Warburton, J., Kincey, M., Johnson, R.M., 2016. Assessment of Torrent Erosion Impacts on the Eastern Flank of Thirlmere Reservoir and A591 (Cumbria) following Storm Desmond 2015, Durham University, Durham.

Watkins, S., Whyte, I., 2008. Extreme flood events in upland catchments in Cumbria since 1600: the evidence of historical records. North West Geography 8(1), 33-41.

Watts, G., Battarbee, R.W., Bloomfield, J.P., Crossman, J., Daccache, A., Durance, I., Elliott, J.A., Garner, G., Hannaford, J., Hannah, D.M., 2015. Climate change and water in the UK–past changes and future prospects. Prog. Phys. Geog. 39(1), 6-28.

Wicherski, W., Dethier, D.P., Ouimet, W.B., 2017. Erosion and channel changes due to extreme flooding in the Fourmile Creek catchment, Colorado. Geomorphology 294, 87-98.

Wilcock, P.R., Crowe, J.C., 2003. Surface-based transport model for mixed-size sediment. Journal of Hydraulic Engineering 129(2), 120-128.

Williams, G.P., 1983. Paleohydrological methods and some examples from Swedish fluvial environments: I cobble and boulder deposits. Geografiska Annaler: Series A, Physical Geography 65(3-4), 227-243.

Williams, G.P., Wolman, M.G., 1984. Downstream effects of dams on alluvial rivers. U.S. Geological Survey Professional Paper 1286. U.S. Government Printing Office, Washington.

Williams, G., Costa, J., 1988. Geomorphic measurements after a flood. In: Baker V.R., Kochel R.C., Patton P.C. (Eds.), Flood Geomorphology. John Wiley and Sons, Canada, pp. 65-80.

Wohl, E., 2015. Legacy effects on sediments in river corridors. Earth-Science Reviews 147, 30-53.

Wolman, M.G., 1954. A method of sampling coarse river-bed material. EOS, Transactions American Geophysical Union 35(6), 951-956.

Wolman, M.G., Gerson, R., 1978. Relative scales of time and effectiveness of climate in watershed geomorphology. Earth Surface Processes and Landforms 3(2), 189-208.